RAIN ATTENUATION CHARACTERISTICS FOR SATELLITE LINKS IN PARTS OF NORTH-EAST AND SOUTH-WEST NIGERIA

BY

SAMUEL ADEIZA VICTOR
MTECH/SPS/2017/7489

DEPARTMENT OF PHYSICS
SCHOOL OF PHYSICAL SCIENCE
FEDERAL UNIVERSITY OF TECHNOLOGY, MINNA NIGERIA

OCTOBER, 2021

ABSTRACT

Characteristics of rain attenuation for Satellite links in three Northeast States (Adamawa, Gombe and Taraba) and three Southwest States (Lagos, Oyo and Ogun) of Nigeria is presented in this work. 33 years (1985 -2017) rainfall data obtainedfrom the Nigerian Meteorological Agency (NIMET) was used**.**Chebil rain rate model was used to compute the point rainfall rate, while the ITU-R P.618-9 model was used to compute the rain attenuation for the six locations. Point rainfall rate of 90.34 mm/h was obtained at Yola while 94.4 mm/h was obtained at Gombe and 96.2 mm/h was obtained at Jalingo. Higher rainfall rates of 108.2 mm/h, 104.8 mm/h and 99.7 mm/h were recorded at Ikeja, Ibadan and Abeokuta respectively. An elevation angles 23°, 42.5° and 55° were considered. Rain attenuation for the Northeastern States ranged between 10.22 dB and 20.24 dB at 55° elevation angle, 11.89 dB to 24.01 dB at 42.5° elevation angle and 19.83 dB to 37.14 dB at 23° elevation angle while the rain attenuation computed for the Southwestern states ranged between 10.60 dB to 22.34 dB at 55° elevation angle, 12.85 dB to 26.44 dB at 42.5° elevation angle and 20.56 dB to 40.99 dB at 23° for exceedance time percentage of 0.01% at Ku-band. For the Ka-band, attenuation varied for the Northeastern States ranged between 33.79 dB and 110.10 dB at 55°elevation angle, 37.88 dB and 121.03 dB at 42.5° elevation angle and between 57.51 dB and 167.19 dB at 23° elevation angle while the rain attenuation computed for the Southwestern states ranged between 44.63 dB and 122.11 dB at 55°elevation angle, 40.39 dB and 133.48 dB at 42.5° elevation angle and between59.71 dB and 183.75 dB at 23° elevation angle for same 0.01% exceedance time percentage in all the stations. From the values of rain attenuation predicted for 0.01% time exceedance, availability of signal is possible at 42.5° and 55° elevation angles but impossible at 23° elevation angle at Ku-band. At Ka-band, the predicted rain attenuation values for 0.01% time exceedance have shown that availability of signal is impossible at all three elevation angles, which implies total signal fade out during such rain fall events in the region.

TABLE OF CONTENTS

Content	Page
Title page	i
Declaration	ii
Certification	iii
Dedication	iv
Acknowledgements	v
Abstract	vi
Table of Contents	vii
List of Tables	xi
List of Figures	xii
List of Plates	xiii
List of Appendices	xiv
List of Abbreviations	xv

CHAPTER ONE

1.0 INTRODUCTION

1.1 Background to the Study	1
1.2 Statement of the Research Problem	3
1.3 Aim and Objectives of the study	3
1.4 Justification of the Research	4
1.5 Significance of the Study	4
1.6 Scope of the Study	4

1.7 Study Area 5

1.7.1 Yola 5

1.7.2 Gombe 5

1.7.3 Taraba 6

1.7.4 Lagos 6

1.7.5 Oyo 7

1.7.6 Ogun 7

CHAPTER TWO

2.0 LITERATURE REVIEW 9

2.1 Rainfall Rate Measurement 9

2.2 Categorisation and Characteristics of Tropical Rainfall 9

2.3 Signal Fading 12

2.4 Causes of Rain Attenuation 13

2.4.1 Absorption 13

2.4.2 Scattering 14

2.5 Conversion of Rain rate to Equivalent 1-minute Integration Time 15

2.6 Rain Rate Prediction Models 17

2.6.1 The rice – holmberg model 17

2.6.2 Chebil and Rahman model 18

2.6.3 Moupfouma and Martin Model 18

2.6.4. The ITU-RP.837-4 model 19

2.7 Rain attenuation models 21

2.7.1 ITU-R Rain Attenuation Model 21

2.7.2 Slant path rain attenuation models 25

CHAPTER THREE

3.0 MATERIALS AND METHODS/ RESEARCH METHODOLOGY 27

3.1 Data Acquisition 27

3.2 Data Analysis 28

3.2.1 Computation of point rainfall rate 28

3.2.2 Calculation of rain-induced attenuation 28

3.2.3 Comparison of rain-induced attenuation 28

CHAPTER FOUR

4.0 RESULTS AND DISCUSSION 30

4.1 Rainfall Data Analysis 30

4.2 Average Rainfall Accumulation for the Study Area 30

4.3 Rain Rate Calculation for the Locations Using Chebil Model 31

CHAPTER FIVE

5.0 CONCLUSION AND RECOMMENDATIONS 60

5.1 Conclusion 60

5.2 Recommendations 61

REFERENCES 62

APPENDICES 65

LIST OF TABLES

Table	Page
4.1Point rainfall rate for the study area	31
4.2 Geographical and experimental parameters for the Northeast Stations	31
4.3 Geographical and experimental parameters for the Southwest Stations	32
4.4 Specific attenuation for horizontal polarisation of the study area (dB/km)	32
4.5 Specific attenuation for vertical polarisation of the study area(dB/km)	33
4.6Specific attenuation for circular polarisation of the study area(dB/km)	33
4.7Horizontal reduction factor for horizontal polarisation of the study area(dB/km)	33
4.8Horizontal reduction factor for vertical Polarisation of the study area(dB/km)	33
4.9Horizontal reduction factor for circular polarisation of the study area(dB/km)	34
4.10Path length for horizontal polarisation of the study area(dB/km)	34
4.11Path length for vertical polarisation of the study area(dB/km)	34
4.12 Path length for circular polarisation of the study area(dB/km)	35
4:13Vertical adjustment factor for horizontal polarisation of the study area(dB/km)	35
4:14Vertical adjustment factor for vertical polarisation of the study area(dB/km)	35
4:15Vertical adjustment factor for circular polarisation of the study area(dB/km)	36
4:16Effective path length for horizontal polarisation of the study area(dB/km)	36
4:17 Effective path length for vertical polarisation of the study area (dB/km)	36
4.18 Effective path length for circular polarisation of the study area (dB/km)	37

LIST OF FIGURES

Figures Page

1.1:36 States of Nigeria with the study area 8

2.1:A schematic diagram of earth-space path 22

4.1.33 years average rainfall for the study area 29

4.2:Rain attenuation at 11GHz and 42.5° for horizontal polarisation for all locations 40

4.3: Rain attenuation at 14 GHz and 42.5° elevation angle for horizontal polarisation41

4.4:Rain attenuation at 20 GHz and 42.5° elevation angle for horizontal polarisation41

4.5: Rain attenuation at 40 GHz and 42.5° elevation angle for horizontal polarisation42

4.6:Rain attenuation at 11 GHz and 42.5° elevation angle for vertical polarisation.42

4.7Rain attenuation at 14 GHz and 42.5° elevation angle for vertical polarisation.43

4.8: Rain attenuation at 20 GHz and 42.5° elevation angle for vertical polarisation43

4.9: Rain attenuation at 40 GHz and 42.5° elevation angle for vertical polarisation44

4.10: Rain attenuation at 11 GHz and 42.5° elevation angle for circular polarisation44

4.11: Rain attenuation at 14 GHz and 42.5° elevation angle for circularpolarisation45

4.12: Rain attenuation at 20 GHz and 42.5° elevation anglefor circularpolarisation45

4.13: Rain attenuation at 40 GHz and 42.5° elevation angle for circular polarisation46

4.14:Rain attenuation at 11 GHz and 55° elevation angle for horizontal polarisation. 46

4.15:Rain attenuation at 14 GHz and 55° elevation angle for horizontal polarisation47

4.16: Rain attenuation at 20 GHz and 55° elevation angle for horizontal polarisation47

4.17: Rain attenuation at 40 GHz and 55° elevation angle for horizontal polarisation48

4.18: Rain attenuation at 11 GHz and 55° elevation angle for vertical polarization 48

4.19: Rain attenuation at 14 GHz and 55° elevation angle for vertical polarization 49

4.20: Rain attenuation at 20 GHz and 55° elevation angle for vertical polarization 49

4.21: Rain attenuation at 40 GHz and 55° elevation angle for vertical polarisation50

4.22: Rain attenuation at 11 GHz and 55° elevation angle for circular polarisation50

4.23: Rain attenuation at 14 GHz and 55° elevation angle for circular polarisation51

4.24: Rain attenuation at 20 GHz and 55° elevation angle for circular polarisation. 51

4.25: Rain attenuation at 40 GHz and 55° elevation angle for circular polarisation. 52

4:26: Rain attenuation at 11GHz and 23° for horizontal polarisation for all locations53

4.27: Rain attenuation at 14 GHz and 23° elevation angle for horizontal polarisation.53

4.28: Rain attenuation at 20 GHz and 23° elevation angle for horizontal polarisation.54

4.29: Rain attenuation at 40 GHz and 23° elevation angle for horizontal polarisation.54

4.30: Rain attenuation at 11 GHz and 23° elevation angle for vertical polarisation.55

4.31: Rain attenuation at 14 GHz and 23° elevation angle for vertical polarisation.55

4.32: Rain attenuation at 20 GHz and 23° elevation angle for vertical Polarisation56

4.33: Rain attenuation at 40 GHz and 23° elevation angle for vertical polarisation56

4.34: Rain attenuation at 11 GHz and 23° elevation angle for circular polarisation57

4.35: Rain attenuation at 14 GHz and 23° elevation angle for circular polarisation57

4.36: Rain attenuation at 20 GHz and 23° elevation angle for circular polarisation58

4.37: Rain attenuation at 40 GHz and 23° elevation angle for circular polarisation. 58

LIST OF PLATES

Plates		**Page**
3.1:	Rain Gauge	27

LIST OF APPENDICES

Appendix **Page**

A: 33 years average rainfall for the study area68

B1: 33 years totalrainfall events for Yola69

B2: Key indicating number representing each month 69

B3: 33 years total rainfall events for Gombe 70

B4: 33 years total rainfall events for Jalingo 71

B5:33 years total rainfall events for Abeokuta72

B6: 33 years total rainfall events for Ibadan73

B7: 33 years total rainfall events for Ikeja 74

C:The Predicted rain attenuation for the study area 75

LIST OF ABBREVIATIONS

ITU-R - International Communications Union Recommendations

GHz - Giga- Hertz (Unit of Frequency)

mm - Millimeter (Unit of Length)

dB - Decibel (Unit of Attenuation)

Km - Kilometer (Unit of Length)

NIMET - Nigerian Metrological Agency

CHAPTER ONE

1.0 INTRODUCTION

1.1 Background to the Study

Atmospheric effects play a major role in the design of satellite-to-earth links operating at frequencies above 10 GHz. The presence of various forms of precipitation such as rain, snow, cloud and fog in radio wave or microwave path is always capable of producing impairment to terrestrial and slant-path communications at these frequencies, but the effect caused by rain is major. Rainfall attenuation can be measured directly on an existing microwave link or it can be obtained indirectly by rain characteristics such as rainfall rate and raindrop size distribution (Crane, 1975). In temperate regions, propagation of radio signals at frequencies above 10 GHz is susceptible to the adverse effects of rain, while even at lower frequencies around 7 GHz, these effects become of greater concern in tropical, sub-tropical and equatorial regions of the world (Moupfouma, 1984), where rainfall is characterised by the high intensity (rain rate), the enhanced frequency of rain occurrence and the presence of large raindrops. The prediction of attenuation events can greatly improve the implementation and effectiveness of fade mitigation techniques (Panagopoulous *et al.*, 2004).

Consumer diversity, demands for bandwidth, and service convergence have led to a tremendous growth in communication systems. These have resulted in congestion at lower frequency bands, and consequently increased the need for higher frequency band usage. Many advantages of telecommunications systems operating at higher frequencies include large bandwidth, increased frequency reuse, small device size and wide range of spectrum

availability; but a major drawback to use of higher frequency bands is attenuation by rain (Malinga *et al.,* 2013). The impacts of rain rate along satellite paths in regions where mixed climate conditions (tropical, sub-tropical and temperate) are common demand special attention with respect to rain attenuation modeling.

Attenuation due to water in the atmosphere varies with density of rain cell and size of the rainfall drops (Freeman, 2013). According to Ivanous and Serdega (2016) attenuation due to absorption is larger than attenuation due to scattering for wavelengths that are small compared with the drop size. For wavelengths that are long compared to drop size, attenuation due to scattering is larger than attenuation due to absorption. While attenuation is caused more frequently by cloud and gases, it is rain that causes the largest attenuation (Omotoso, 2008; Adrian, 2011). The influence of attenuation due to hydrometeors increases with increasing operating frequency (Malinga *et al.*, 2013).

The magnitude of attenuation caused by rain depends on parameters such as the size of raindrops, rain temperature, drop velocity, polarisation, rain rate, drop orientation and transmitting frequency (Malinga *et al.*, 2013). Hydrometeors can introduce significant attenuation and depolarisation through their ability to absorb and scatter radio waves (Shoewu and Edeko, 2013; Emiliani, 2014).

Rain also depolarises satellite signals, converting energy from one polarisation to another, and causing interference between channels that depend on orthogonal polarisation for frequency reuse. At C- and K-bands rain depolarisation must be taken into account in dual-polarised systems (Tokay and Short, 2015).

1.2 Statement of Research Problem

It is rain that has the most deleterious effect on radio signal propagation at frequencies beyond 10 GHz, hence, rain attenuation is the major setback in the design of wireless networks that are highly reliable and perform optimally. Such signal attenuation comes with varying degrees of severity depending on the intensity, raindrop size, rain rate and the frequency of operation. High rain rates have significant adverse effects on radio links and often cause complete signal outages (total unavailability of service). Thus, there is a need to predict accurately the amount of attenuation caused by rain on both terrestrial and satellite links in given environments. Although many researchers both in the past and recently have studied rain attenuation in Nigeria and other parts of the world, it is hardly enough and is not conclusive in any way. Thus, the results from this work will complement the existing ones and assist satellite designers in producing more accurate systems required for the study area.

1.3 Aim and Objectives

The aims of this work is to study rain attenuation characteristics for satellite links in parts of

North-east and South-west Nigeria.

The objectives are to:

i. convert daily rainfall accumulation data to point rainfall rate.
ii. predict rain attenuation at Ku and Ka frequency bands.
iii. compare the extent of rain attenuation in the study area for different polarisations.

1.4 Justification of the Research

This reseach work will provide information on rainfall rate and rain attenuation values peculiar to the stations, which may guide radio propagation research in the locality. The knowledge gained will assit earth-space communication engineers and radio physicists to build on link budgets analysis and the quality of communication systems they use with a view to identify attenuation margins to be used for better communication systems design and also provide data on rainfall rate and rain attenuation characteristic for satellite links in parts of northeast and southwest Nigeria.

1.5 Significance of the Study

This thesis would give an insight regarding to rainfall rate and rain attenuation values in the locations, which will help satellite communication engineers in designing communication equipment that will suit the study area.

1.6 Scope of the Study

This work employ rain data from the Nigerian Meteorological Agency (NIMET) for a period of 33 years to deduce rain attenuation along satellite -to- Earth propagation links at Ku, and Ka frequency bands over Adamawa, Gombe, Taraba, Lagos, Ogun and Oyo States in Nigeria.

1.7 Study Area

1.7.1 Yola

Yola is the capital city and administrative centre of Adamawa State, located on the Benue River. It lies on the geographical coordinates of 8° 29' 0" N, 10° 34' 0" E. Generally, the climate of Yola is tropical. The wet season here has a good deal of rainfall, while the dry

season has very little. According to Köppen and Geiger, this climate is classified as Aw (tropical wet). The average annual temperature is 28.0 °C in Yola. In a year, the average rainfall is 933 mm (http://en.wikipedia.org).

1.7.2 Gombe

Gombe is the capital city of Gombe State, north-eastern Nigeria. It is on latitude: 10°16′60.00″N, Longitude: 11° 09′ 60.00″E with a land area of 20,265 Square km (Gombe State Diary 2006). The climate is characterised by a dry season of six months, alternating with a six months' rainy season with an average rainfall of 850 mm (htt://en.Wikipedia.org). By October, the amount of rainfall begins to decrease (Yahaya, 2015). The mean annual temperature is about 32°C. Weather tends to be very hot

between November and March with average temperature that can exceed 32°C or more. The hamattan wind from around February makes the temperature cooler, although with dusty conditions, whereas relative humidity has some pattern being 90% in August and dropping to less than 10% during the hamattan period (Balzerek *et al.*, 2003).

1.7.3 Taraba

Taraba is one of the north-eastern states in Nigeria, named after the Taraba River which traverses the southern part of the State. Taraba's capital is Jalingo, with an estimated land area of about 54,428 Square km, the State lies roughly between latitudes 6° 25′N and 9° 30′N and between longitudes 9°30′E and 11°45′E. Taraba is bounded in the west by Nasarawa State and Benue State and in the north-west by Plateau State. It is also bounded in the north by Bauchi State and Gombe State, in the north-east by Adamawa State, and in the east and south by Cameroon. Taraba has an average rainfall of 800 mm (http://en.wikipedia.org).

1.7.4 Lagos

Lagos is the capital of Lagos State in Nigerian. The city, with its adjoining conurbation, is the most populous in Nigeria. It is one of the fastest growing cities in Africa and one of the most populous urban areas.The State is sharing its name with the city of Lagos, Nigeria, the second largest city in Africa, which lies on its south-western side. It lies on Latitude: $6^{\circ}27`14.65"N$ Longitude: $3°23'40.81"E$. Lagos experiences a tropical savanna

climate according to the Köppen climate classification, as there's a significant precipitation different between the wet season and the dry season, with an average rainfall of 1506.6 mm (http://en.wikipedia.org).

The wet season starts in April and ends in October, while the dry season starts in November and ends in March. The wettest month is June with a precipitation total of 315.5 millimetres (12.42 in), while the driest month is January with a precipitation total of 13.2 millimetres.

1.7.5 Oyo

Oyo, usually referred to as Oyo State to distinguish it from the city of Oyo, is an inland State in south-western Nigeria, with its capital at Ibadan. It lies on Latitude: 8° 7.174'N, Longitude: 3° 25.1732'E. It is bounded in the north by Kwara State, in the east by Osun State, in the south by Ogun State and in the west partly by Ogun State and partly by the Republic of Benin. The Climate is equatorial, notably with dry and wet seasons with relatively high humidity. The dry season lasts from November to March while the wet season starts from April and ends in October. According to Köppen and Geiger, the climate is classified as Aw. Average daily temperature ranges between 25 °C (77.0 °F) and 35 °C (95.0 °F), almost throughout the year. Oyo state has an average rainfall of 1190mm (http://en.wikipedia.org).

1.7.6 Ogun

Ogun State is a state in southwestern Nigeria. Created in 1976, it borders Lagos State to the south, Oyo and Osun states to the north, Ondo to the east and the Republic of Benin to the west. It lies on Latitude 6° 54'.59"N, Longitude 3° 15'.5018" E. Abeokuta is the capital and largest city in the state. It was created in February 1976 from the former Western Nigeria State. This city has a tropical climate. Most months of the year are marked by significant rainfall. The short dry season has little impact. According to Köppen and Geiger, the climate is classified as Aw. The temperature here averages 27.1 °C, while the average annual rainfall is 2152 mm

(http://en.wikipedia.org).

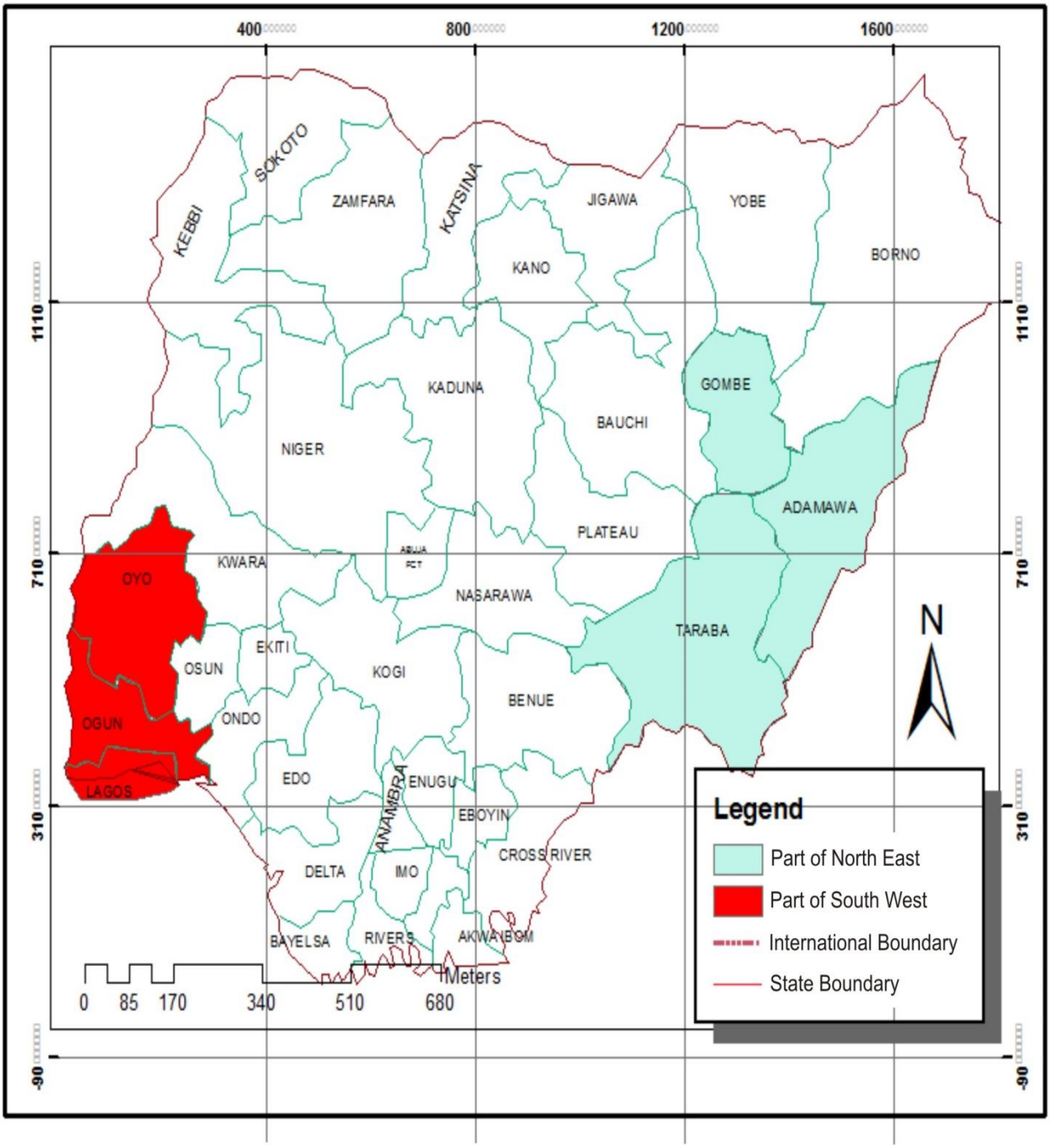

Figure 1.1: 36 States of Nigeria with the study area
Source: Ministry of land and Housing with Authors' modification

CHAPTER TWO

2.0 LITERATURE REVIEW

2.1 Rainfall Rate Measurement

Traditionally, attenuation is expressed in terms of rainfall rate using a power-law relationship (Rahim *et al.,* 2013). Conversely, this relationship can be used to determine rainfall rate from link attenuation. The power-law is generally considered to be a good representation of the relationship between attenuation and rainfall (A-R). However, since the power-law relationship is potentially non-linear, it is not always possible to estimate true average rainfall from path average attenuation. The International Telecommunication Union of Radio Communications (ITU-R) sector provides a standard definition to calculate specific attenuation from rainfall rate based on the power-law relationship using ITU-R.P.838-3 (ITU-R, 2013). The coefficients of the A-R relationship are also highly dependent on the raindrop size distribution (DSD), which can vary significantly (Emiliani, 2014). The frequency threshold in temperate climates is about 10 GHz. In tropical and equatorial climates, due to higher rainfall and larger raindrop sizes than in temperate climates, the incidence of rainfall on radio links becomes important for frequencies as low as about 7 GHz (Moupfouma and Tiffon, 2014).

2.2 Categorisation and Characteristics of Tropical Rainfall

Rainfall is broadly classified into two types. They are Stratiform (drizzle and widespread) and Convection (shower and thunderstorm). The drizzle is a type of rain which consists entirely of small rain drops usually of diameter less than 1 mm and commonly falls in damp

weather from shallow layer clouds. It is characterised by very low rainfall rates with typical values not greater than 5 mm/h. The widespread rain is associated with stratiform clouds. It is developed by sublimation through coalescence process. It consists largely of medium rain drops of diameter ranging from 1 to 2.5 mm. Widespread rain events usually have intensity between about 9 – 25 mm/h and the intensity may be practically constant or change only gradually during precipitation. The duration of widespread rain event may be several hours. This type of rain may sometimes extend to the Zero Degree Isotherm (ZDI) height since the ice phase is involved (Ajewole, 2011).

The shower type of rain on the other hand originates from cumuliform clouds. This type of rain is characterised majorly by high intensity values, ranging from about 50 mm/h to about 120 mm/h and with raindrops of diameter greater than 2 mm. The fall duration of shower precipitation is about 10 – 15 minutes. It is formed below the Zero Degree Isotherm (ZDI) height through the process of accretion. Its formation is due largely to the rate of accretion, the thickness of clouds, and the strength of the up draughts (Ajewole, 2011). The shower and thunderstorm rain types usually occur over very limited horizontal extent typically of 1 – 2 km and are therefore localised. They have the most effect on terrestrial and Earth-space communications links, especially in tropical locations (Ajewole, 2011).

The thunderstorm rain is usually generated within the cumulonimbus cloud systems (Hassen, 2014). It consists of one or more active cells containing strong vertical air currents. These are usually the Centre of raindrop and lightning activities. Each rain cell goes through a life cycle of growth, maturity and decaying stages when lightning occurs. During thunderstorm activity, the precipitation particles grow in size until they grow large

to become drops of diameter greater than about 3 mm and are no longer supported by the upward currents. At this stage, they fall to the ground with values of rain rate between about 50 mm/h and 240 mm/h in tropical locations (Adimula, 2015). At maturity, as columns of cooled air sink to the ground with strong down drafts and horizontal wind, electrical charges accumulate on cloud particles and lightning occurs. The lightning heats the air producing huge intense shock waves and rumbling observed as thunder. Ojo and Olurotimi (2017) studied spatial variability of rainfall structure in two locations (Akure and Lagos) in southern Nigeria using 2years of measured rainfall data of 1-minute integration time to investigate the propagation effects on microwave and millimeter-wave communication systems. It was observed that the rain forest region (Akure) and the coastal region (Lagos) both recorded their peak average monthly rainfall accumulation in the same month when the worst month was experienced. Comparison of measured data with ITU-R data shows that the recent ITU-R model overestimated the rainfall rate at 0.01% exceedence of time by about 21% for Akure, while it was underestimated by about 31% for Lagos. The results of threshold of rainfall illustrated higher numbers in Lagos when compared with Akure and that the lower rainfall rates contributed the most to the thresholds. Dependence of average rain rate on the duration of rain event shows that in Akure, the average rainfall intensity during the rain events is about 8.59 mm/h, the maximum rainfall intensity during rain events was 179.6 mm/h, while in Lagos the minimum rainfall intensity during rain events was 1.51 mm/h and the maximum rainfall intensity was 206.8 mm/h. The frequency of occurrence in the early hours of the day is higher in Lagos when compared with Akure. These hours comprise the period for which communication services, like transaction of businesses through internet, telephony, electronic banking and so on take place; while in the evening hours people are expected to

enjoy direct-to-home television services. System engineers therefore need to take into cognisance, the rainfall rate variations bearing in mind the volume of commercial activities taking place in the two cities (Lagos is the main industrial and commercial capital of Nigeria, while Akure is the capital city of Ondo state, Nigeria.

Akinyemi *et al.,* (2018) evaluated the characteristics of the satellites of Nigeria Communication Satellite (NIGCOMSAT-R1), which operates on C-, Ku- and Ka-bands but projections are made into the V-band. Across all frequency bands, rainfall attenuation and effective path length have been determined for satellite links in Nigeria. Considerations were made for link availabilities from 95% up to 99.99% of the time. It is noted that for a particular given percentage availability, attenuation increases with effective path length as well as the frequency of operation. It is noted also, that the severity of the degradation of the propagating signal increases with increasing availability. For a given location, the effective path length varies directly with the frequency.

2.3 Signal Fading

The most troublesome and frustrating problem in receiving radio signals is variations in signal

strength, most commonly known as fading. The attenuation may vary with time, geographical

position or radio frequency, and is often modeled as a random process. Fading may either be due

to multipath propagation, referred to as multipath induced fading, or due to shadowing from

obstacles affecting the wave propagation, sometimes referred to as shadow fading.

There are several conditions that can produce fading. When a radio wave is refracted by the

ionosphere or reflected from the Earth's surface, random changes in the polarisation of the wave

may occur. Vertically and horizontally mounted receiving antennas are designed to receive

vertically and horizontally polarised waves, respectively. Therefore, changes in polarisation

cause changes in the received signal level because of the inability of the antenna to receive

polarisation changes.

Rain attenuation is usually estimated experimentally and also can be calculated theoretically

using scattering theory of rain drops. Rain drop size distribution (DSD) is an important

consideration for studying rain attenuation characteristics. Various mathematical forms such as

Gamma function, or exponential forms are usually used to model the DSD. Mie or Rayleigh

scattering theory with point matching or t-matrix approach is used to calculate the scattering

cross section, and specific rain attenuation. Since rain is a non-homogeneous process in both time and space, specific attenuation varies with location, time and rain type (https://en.wikipedia.org/wiki/Rain_fade). Total rain attenuation is also dependent upon the

spatial structure of rain field. Horizontal and vertical extensions of rain again vary for different

rain types and location. Limit of the vertical rain region is usually assumed to coincide with 00

isotherm and called rain height. Melting layer height is also used as the limits of rain region and

can be estimated from the bright band signature of radar reflectivity.

The horizontal rain structure is assumed to have a cellular form, called rain cell. Rain cell sizes

can vary from a few hundred meters to several kilometers and are dependent upon the rain type

and location. Existence of very small size rain cells are recently observed in tropical rain (https://en.wikipedia.org/wiki/Rain_fade). Possible ways to overcome the effects of rain attenuation are site diversity, uplink power control, variable rate encoding, receiving antennas

larger (i.e. higher gain) than the required size for normal weather conditions.

2.4 Causes of Rain Attenuation

Any satellite communications system network operator using a Ku-Band system (12/14 GHz or

higher frequencies) will face the effects of rain fade at some time. But to understand why this

weakening occurs with higher frequencies, knowledge of the causes of rain fade is important.

Two of the most common causes are as follows.

2.4.1 Absorption

Part or all of the energy generated when a radio wave strikes a rain droplet is converted to

heat energy and absorbed by the droplet.

2.4.2 Scattering

A non-uniform transmission medium (the raindrops in the atmosphere) causes energy to be
dispersed from its initial travel direction. Scattering can be caused by either refraction or diffraction:

i. Refraction

Refraction is the change in direction of propagation of a wave due to a change in its transmission
medium (Wikipedia). This occurs when signal travels through one medium to another especially
when both media have different refractive indices. In other words, the refractive index of the
water droplet encountered by radio wave causes it to be refracted. The refractive index of water
is dependent on both temperature and frequency.

ii. Diffraction

Diffraction is a term used to describe the phenomenon of electromagnetic waves bending around

obstacles (Wikipedia). When a radio wave encountered a water droplet, the travel direction of

the radio wave changes as it propagates around the water droplet (obstacle) in its path

These different reactions ultimately have the same effect they cause any satellite system to lose

some of its normal signal level. Rain outage will only occur during the heaviest rains (convective and straitform are the most pre-dominant types) with only a small portion of the transmission path experiencing attenuation.

2.5 Conversion of Rain rate to Equivalent 1-minute Integration Time

The International Telecommunication Union (ITU) has created a statistical model in which the Earth is divided into 15 different rain zones, where each zone corresponds to a certain level of rain rate. In most tropical locations including Nigeria, there is dearth of rainfall rate of 1-minute integration time. Ajayi and Ofoche (1984) developed 1-minute rain rate map for Nigeria using Rice-Holmberg model. Ojo and Ajewole (2011) worked on dimensional statistics of rainfall signature and fade duration for microwave propagation in Nigeria. The authors were able to establish that at higher time percentages up to 0.2% for higher frequencies of 30 GHz, the values of attenuation obtained are higher than the values of rain rate that produce it. The results however overestimated rain rate for the high availability time requirement of 0.01%, and underestimated rain rate for the low availability time requirement between 0.1 to 1%. Khandaker and Mohammad (2014)

studied the performance analysis of rain fades on microwave earth-to-satellite links in Bangladesh. One-minute integration time rain intensity data were derived from thirteen years' annual rainfall statistics measured at 34 meteorological stations in Bangladesh. The converted rain intensity data were used to estimate rain fades at C, Ku and Ka bands, but did not treat other areas of fade dynamics like the fade duration and the fade slope. Ojo *et al., (*2015) employed the Moupfouma and Martins (2015) model purposely designed for tropical locations to convert rain rate to the 1-minute equivalent for Nigeria and got results that show that in South-South region, the cumulative distribution of rain rate is approximately about 130 mm/h for the high availability time requirement of 0.01%, while it is about 50 mm/h for the low availability requirement of 0.1%. This is lower than the values (145 mm/h for 0.01% and 65 mm/h for 0.1%) predicted by ITU-R for the coastal regions of Nigeria. From Sokoto in the arid north-west through Katsina to Maiduguri in the north-east, rain rates varies from about 65 to 80 mm/h for the high availability requirement and approximately 30 mm/h for the low time availability requirement of 0.1%. These values strongly contrast the values of 95 mm/h and 35 mm/h respectively for the 0.01% and 0. 1% time availability predicted by the ITU-R for the arid regions of Nigeria (ITU ZONE N). The gross overestimation by the ITU – R model is obvious. Several efforts have been made by many researchers to estimate the level of degradation of terrestrial and satellite signals in Nigeria. Omotosho (2016) investigated the effects of propagation impairments such as due to rain, cloud, gases and tropospheric scintillation on fixed satellite communication link on earth-space path for frequencies between 10 and 50 GHz i.e at Ku, Ka and V bands for 37 locations in Nigeria. Elevation angles of 50^0 and 55^0 of Nigeria Communication Satellite, (NigComsat-1) were used in the computation of the propagation impairments for the 37 locations. The International Telecommunication

Union Radiowave Propagation models (ITU-RP) were used in the investigation of the propagation impairments. The author concluded that Tropospheric scintillation is very high in the south-south region and combined impairments due to multiple sources of simultaneously occurring atmospheric attenuation is severe in south-east. Overall, Sokoto and Katsina appear as good locations to site fixed satellite earth stations operating at Ku band and above. Islam *et al.,* (2018) predicted the attenuation due to rain accurately, rainfall intensity is required with 1-minute integration time. Rain intensity with 1-minute integration time were measured for 6 years at IIUM Kuala Lumpur campus in Malaysia. Monthly and yearly statistical distributions of measured rain rates are presented. Moupfouma, Crane and ITU-R models for rain rate distributions are compared with measured rain rates. All models overestimate the measurements most of time in measured year. It is observed for 0.01 percentage of time, measured six years average rain rate is 110 mm/h, while 135, 147 and 145 mm/h are predicted by Global Moupfouma, Crane and ITU-R models for Malaysia. At 0.01% of time, the measured rain rate is found to be 110 mm/h while ITU-R latest recommendation has proposed 100 mm/h rain.

Igwe *et al.,* (2019) evaluated some rain attenuation prediction models for satellite communication at Ku and Ka bands. It was observed that rain attenuation at Ka-band (19.45 GHz) is significantly higher than at Ku-band (12.675 GHz) for all the elevation angles. The predicted rain attenuation by ITU-R model exceeded for 0.001 % of the time is as high as 52 dB, 54 dB and 75 dB at 55°, 42.5° and 23° respectively. Also, at 0.01 % of time, the rain attenuation predicted varies between 37 dB and 47 dB at the Ka-band frequency for the three elevation angles.

2.6 Rain Rate Prediction Models

2.6.1 The Rice – Holmberg Model

Rain rate models are used to predict the rainfall-rate cumulative distribution of any location. Several of such models exist. However, some of them have one discrepancy or the other (Ryde, 1946), this model overestimates rain rates in the high availability range of 0.01% and underestimates rain rates in the low availability range of 0.1% and 1%. Rice and Holmberg (1973) developed a model for obtaining rain rate values for use in fade calculations. The model required parameters like the highest monthly rainfall accumulation observed in a set of 30-year period, number of thunderstorm days expected in an average year and the average annual accumulation. The limitation is that the thunderstorm ratio is not readily available from local weather agencies. Also the number of stations and data available is few, and not all the stations satisfy the one-minute integration time requirement (Crane, 1982); some require a relatively high density of short integration time (Khandaker and Mohammad, 2014).

2.6.2 Chebil and Rahman Model

Chebil and Rahman (1999) proposed a model which is used to convert the rain amount data of any location to its equivalent rain rate data irrespective of the integration time of the available rain data. It uses a long-time mean annual accumulation, M, of rain collected for the location under studied and it was expressed by (Chebil and Rahman 1999):

$$R_{0.01} = \alpha M^{\beta} \tag{2.1}$$

where α and β are regression coefficients given as α= 12.2903; and β= 0.2973, M is the total rain fall measured for a year and rain rate $R_{0.01}$is measured in mm/h.

2.6.3 Moupfouma and Martin Model

Recent analysis suggests that rain rate distribution is better described by a model which approximates a log-normal distribution at low rate and a gamma distribution at high rate. The model was developed by Moupfouma and Martin (1995). This model known as the Moupfouma and Martin's rain rate model is good for both tropical and temperate regions. It is expressed by Moupfouma, (2009) as:

$$P(R \geq r) = 10^4 \left(\frac{R_{0.01}}{r+1} \right) b \exp\left(\mu \left[R_{0.01} - r \right]\right)$$

(2.2)

where P is the probability of a rain event at 0.01% of the time, r (mm/h) represents the rain rate exceeded for a fraction of the time, $R_{0.01}$ (mm/h) is the rain intensity exceeded during 0.01% of time in an average year and b is approximated by the expression (Moupfouma, 2009);

$$b = \left(\frac{r - R_{0.01}}{R_{0.01}} \right) ln \left(\frac{1+r}{R_{0.01}} \right)$$

(2.3)

The slope of the rain cumulative distribution is governed by the parameter μ, which depends on the local climate conditions and geographic features. For tropical and subtropical regions,

$$\mu = \left(\frac{4\ln 10}{R_{0.01}} \right) \exp\left(-\lambda \left[\frac{r}{R_{0.01}} \right] \gamma \right)$$

(2.4)

λ and ϒ are positive constants and are given as λ = 1.066, ϒ =0.214 and $R_{0.01}$ is the rain rate exceeded for 0.01% of time and is obtained using Chebil and Rahman (1999) model. Thus the refined Moupfouma model can be used to determine the one-minute rain rate cumulative distribution from the long term mean annual rainfall rate.

2.6.4. The ITU-RP.837-4 Model

Another rain rate prediction model is the ITU-R recommended model, which depends on the Salonen - Baptista model (Salonen and Poiares-Baptiste, 1997). It is used to calculate the rain rate at a given location based on the geographic coordinates. ITU-R Recommendations P1144-3 and P837-4 are combined to obtain the rain rate (mm/h). The ITU-P 837-4 model requires as input the following parameters:

Ms defined as the mean annual stratiform rainfall amount (mm)

Mc defined as the mean annual convective rainfall amount (mm) and

Pr_6 defined as the probability of a given rainy period (%).

ITU has the parameters given mapped out all over the world using 15 years of re-analysis products of the European center for medium range weather forecasts (ECMWF ERA 15 data set).

To obtain rain rate using ITU model, the following steps are adopted:

STEP 1

The variables Pr_6, Ms and Mc are extracted for the four points closest in latitude (Lat.) and longitude (Lon.) to the geographical coordinates of the location under study.

STEP 2

From the values of Pr_6, Ms and Mc at the four grid points, the values Pr_6 (Lat, Lon), Mc (Lat.,

Lon) and Ms (Lat., Lon) are obtained by performing bi-linear interpolation Given values at four surrounding grid point: I(R, C); I(R,C+1); I(R+1, C) and I(R+1, C+1), I(r, c) can be obtained when r is a fractional row number and c is a fractional column number using bi-polar interpolation as ((ITU- R,2013)):

I(r,c)=I(R,C)[(R+1- r)(C+1-c)]+I(R+1,C)[(r-R)(C+1-c)]+I(R,C+1)[(R+1-r)

(2.5)

where R, C, r, c are values at four surrounding grid points of the location under study.

STEP 3

The percentages of probability (P_0) of rain in an average year are obtained from (ITU, 2013)

$$P_0(Lat.Lon) = P_{r6}(Lat..Lon)\left(1 - e^{-0.0079(M_s(Lat.Lon)\backslash P_{r6}(lat.Lon)}\right)$$

(2.6)

If P_{r6} is equal to zero, the percentage probability of rain in an average year and the rainfall rate exceeded for any percentage of an average year are equal to zero. In this case, the preceding steps are unnecessary.

2.7 Rain Attenuation Models

Various methods were developed for the calculation of cumulative distributions (CDs) of attenuation due to rain from rain intensity measurements (COST 235, 1996; ITU-R, 2009). Rain attenuation exceeded at 0.01% of the time of the year is calculated from the average 1-minute rain intensity exceeded at the same time percentage. The value obtained is scaled by the empirical formula to other percentages of time between 1% and 0.001% (Vaclav and Martin, 2007).

2.7.1 ITU-R Rain Attenuation Model

In this section, a rain attenuation model is presented that has performed well for many regions and different rain types. This rain attenuation model is the ITU-R model, which is the most widely accepted international method and benchmark for comparative studies. This model is semi- empirical and often employs the local climatic parameters at a desired probability of exceedance.

The ITU-R 618-10 gives summarised procedures for the computation of a satellite path rain attenuation. In order to compute the slant-path rain attenuation using point rainfall rate, the following parameters are required:

F is the frequency of operation in GHz, μ is the elevation angle to the satellite, in degrees, *Á* is the latitude of the ground station, in degrees N and S, *hs*: the height of the ground station above sea level, in km,

Re: effective radius of the Earth (8500 km),

$R_{0.01}$: point rainfall rate for the location of interest for 0.01% of an average year (mm/h).

Figure 2.1: Show a schematic diagram of earth-space path giving the parameters to be inputted into the attenuation prediction process (ITU-RP 618, 2012).

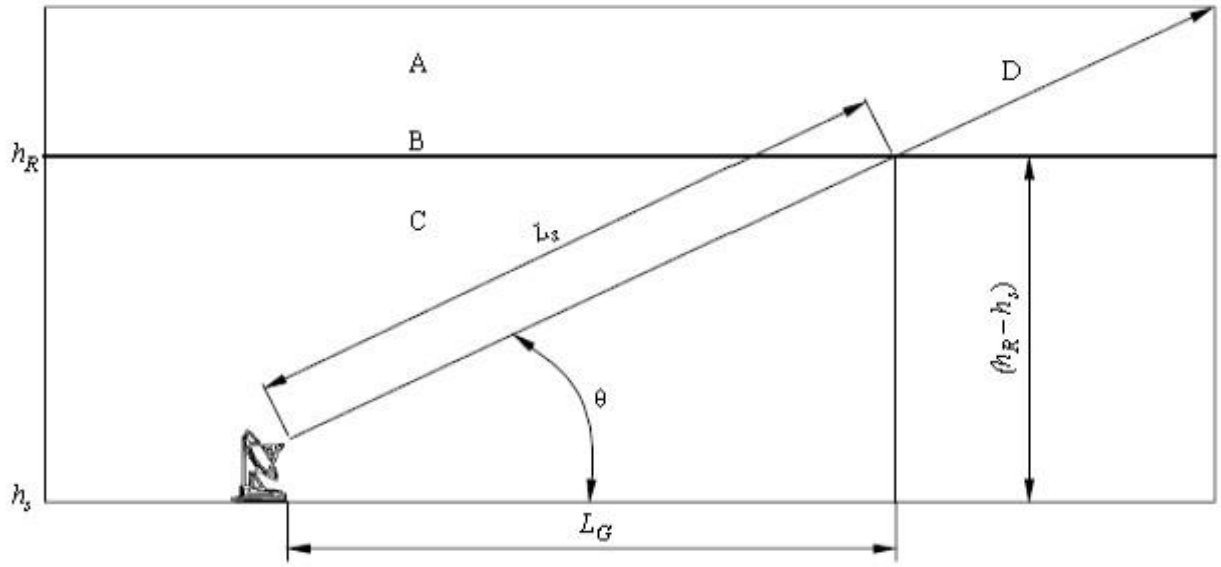

Figure 2.1: A schematic diagram of earth-space path giving the parameters to be inputted into the attenuation prediction process (ITU-RP 618, 2012).

where

A: Frozen precipitation

B: Rain height

C: Liquid precipitation

D: Earth-space path

Step-by-step procedures for the computation of the rain attenuation along the slant-path of a satellite system are summarised as follows:

Step 1: Determine the rain height, h_R .

Step 2: Determine the slant-path length and the horizontal projection.

The slant-path length L_S , expressed in km, is calculated from:

$$L_s = \frac{(h_R - h_s)}{\sin\theta} \quad \text{km} \tag{2.7}$$

For $\theta < 5°$, the following formula is used

$$L_s = \frac{2(h_R - h_s)}{\left(\sin^2\theta + \right)\frac{2(h_R - h_s)^{1\backslash 2}}{R_e} + \sin\theta} \quad \text{km} \tag{2.8}$$

Step 3*:* Calculate the horizontal projection, *LG*, of the slant-path length from:

$$L_G = L_S \cos\theta \quad \text{km} \tag{2.9}$$

Step 4: Determine the rain rate at 0.01% for the location of interest over an average year. In this work, derived rain rate integration time at 0.01% of exceedance from data collected from NIMET stations is given as:

$$R_{0.01} = \alpha M^{\beta} \tag{2.10}$$

where α and β are regression coefficients defined as: α = 12.2903; and β = 0.2973

Step 5: Obtain the specific attenuation, γR, using the frequency-dependent coefficients given in Recommendation ITU-R P.838 and the rainfall rate, $R_{0.01,}$, determined from Step 4, by using:

$$\gamma R = k(R_{0.01})^{\alpha} \quad \text{dB\km} \tag{2.11}$$

Step 6*:* Calculate the horizontal reduction factor, $r_{0.01}$, for 0.01% of the time:

$$r_{0.01} = \frac{1}{1 + 0.78\sqrt{\frac{L_G \gamma R - 0.38\left(1 - e^{-2L_G}\right)}{f}}}$$

(2.12)

Step 7: Calculate the vertical adjustment factor, $V_{0.01}$, for 0.01% 0f the time

$$\zeta = Tan^{-1}\left(\frac{h_R - h_S}{L_G r_{0.01}}\right) \quad \text{degrees}$$

$$For \zeta > \theta, L_R = \frac{L_G r_{0.01}}{\cos\theta} \quad \text{km}$$

Else, $$L_R = \frac{\left(h_R - h_S\right)}{\sin\theta} \quad \text{km}$$

If $|\varphi| < 36°$, x = 36 - $|\varphi|$ degrees

Else, x = 0 degree

$$V_{0.01} = \frac{1}{1 + \sqrt{\sin\theta \left(31\left(1 - e^{-(\theta/(1+x))}\right)\frac{\sqrt{L_R \gamma_R}}{f^2} - 0.45 \right)}}$$

(2.13)

Step 8: The effective path length is:

$$L_E = L_R V_{0.01} \quad \text{km}$$

(2.14)

Step 9:The predicted attenuation exceeded for 0.01% of an average year is obtained from:

$$A_{0.01} = \gamma R L_E \quad \text{dB}$$

(2.15)

Step 10: The estimated attenuation to be exceeded for other percent

ages of an average year, in

the range 0.001% to 5%, is determined from the attenuation to be exceeded for 0.01% for an

average year:

If P $\geq$ 1% $or|\varphi| \geq 36°$ $\beta = 0$

If P < 1% and $|\varphi| < 36°$ $and\ \theta \geq 25°$: $\beta = -0.005(|\varphi| - 36)$

Otherwise: $\beta = -0.005(|\varphi| - 36) + 1.8 - 4.25\ sin\theta$

$$A_P = A_{0.01}\left(\frac{p}{0.01}\right)^{-\left(0.655+0.033\ln(p)-0.045\ln(A_{0.01})-\beta(1-p)\sin\theta\right)} \text{ dB.}$$

(2.16)

where

$$\beta = \begin{Bmatrix} 0 if \geq 1\% or / \varphi / \geq 36° \\ -0.005(/ \varphi / - 36°) if, p < 1\% and / \varphi / < 36° and \theta \geq 25° \\ -0.005(/ \varphi / - 36°) + 1.8 - 4.25\sin\theta, otherwise \end{Bmatrix}$$

This method provides an estimate of the long-term statistics of attenuation due to rain.

2.7.2 Slant Path Rain Attenuation Models

Rain attenuation can either be obtained directly from microwave link measurements or estimated from the rain rate and rain drop-size distribution data. Ajayi *et al.,* (1990) provided a methodological approach for estimating rain-induced attenuation from available precipitation data (rain statistics), using method of moment of regression to estimate the number of drop size, and compared the results with log-normal distribution. This model is semi- empirical and often employs the local climatic parameters at a desired probability of exceedance (Parth and Rutvij, 2016.

CHAPTER THREE

3.0 RESEARCH METHODOLOGY

3.1 Data Acquisition

The meteorological data used for this research work were acquired from the Nigerian Meteorological Agency (NIMET), Abuja for the Northeastern region (Yola, Gombe and

Jalingo) and Southwestern region (Ikeja, Abeokuta and Ibadan). The daily rainfall data was measured for a period of 33 years (January, 1985 to December, 2017).

Plate 3.1: Shows a sample rain gauge



Plate 3.1: Rain Gauge

3.2 Data Analysis

3.2.1 Computation of Point Rainfall Rate

The rainfall data of 33 years was analysed and averaged to one year. Chebil rain rate model was used to compute the point rain rate for the locations using equation (2.1).

3.2.2 Calculation of Rain-induced Attenuation

The ITU-R P. 618-2012 model was used to calculate the rain-induced attenuation as given in equations (2.7 - 2.16) by following the step by step procedures.

One of the vital input for the recommendation is the point rainfall rate for the location for 0.01% of an average year (mm/h) obtained from Chebil rain rate model. Other input parameters for the model are:

h_s: height above the mean sea level of the earth station (km)

Θ: elevation angle (degrees)

φ: latitude of the earth station (degrees)

f: frequency (GHz)

R_e: effective radius of the earth (8500)

This procedure provides an estimate of the long-term statistics of attenuation due to rain at a given location for higher frequencies.

3.2.3 Comparison of Rain-induced Attenuation

The calculated rain-induced attenuation was done at different frequencies (Ku and Ka-bands) and at different polarisation (vertical, circular and horizontal) in order to determine the polarisation type that has the least to the highest rain-induced attenuation.

CHAPTER FOUR

4.0 RESULT AND DISCUSSION

4.1 Rainfall Data Analysis

The total rainfall data for a period of 33 years (January, 1985 to December 2017) of both rainy and dry days for the six stations (Adamawa, Gombe, Taraba, Lagos, Ogun and Oyo States) in Nigeria considered for this study has been analysed .The statistical data representing the details of the six stations is shown in Figure 4.1

4.2 Average Rainfall Accumulation for the Study Area

4.2.1 33 years average rainfall for the study area

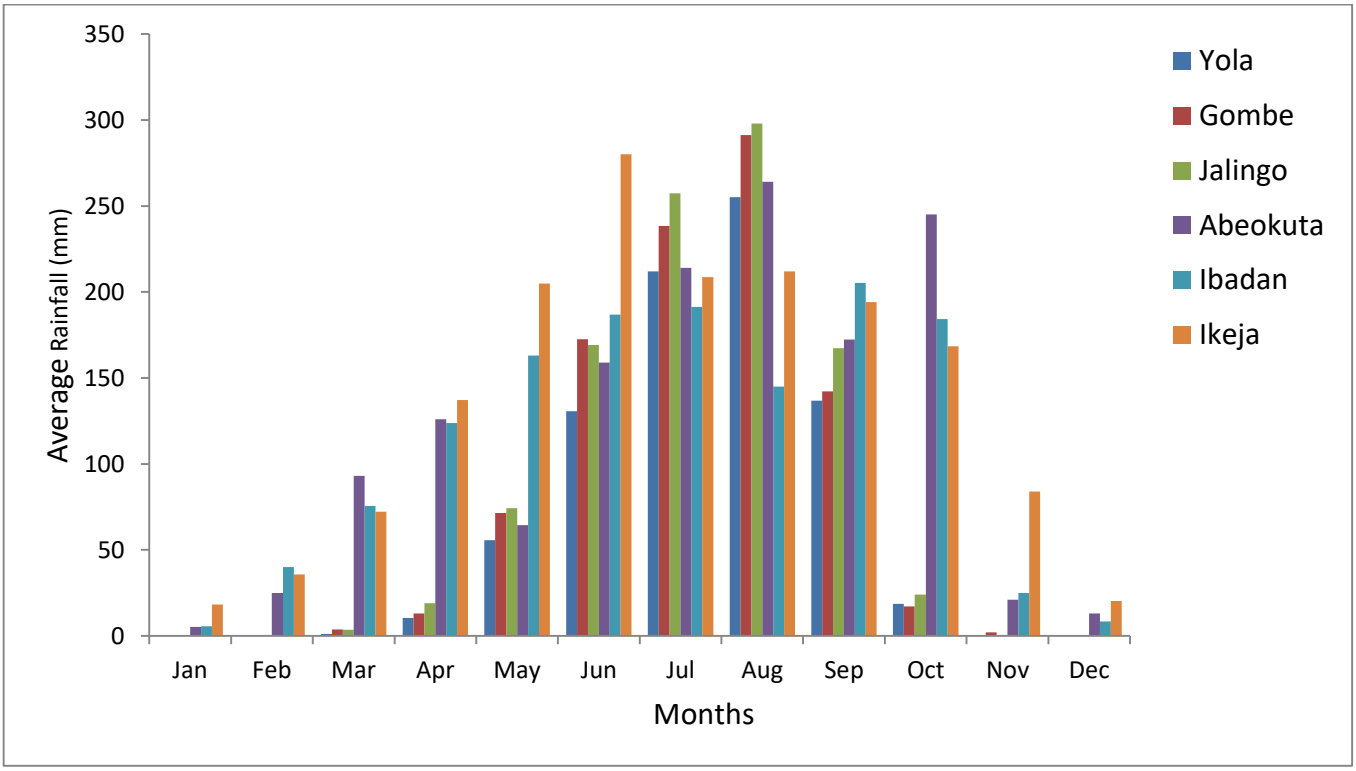

Figure 4.1: A 33-year monthly average rainfall for the study areas

The average rainfall for 33 years for the study area is shown in figure 4.1. For the entire period, rainfall in Adamawa, Gombe and Taraba was generally low during the dry season (November–March) while the wet season (April–October) expectedly recorded higher amount of rainfall. Jalingo (in Taraba State) had the highest average rainfall of 297.9 mm in August, while Gombe recorded the highest amount in the month of August with 291.2

mm. Yola (in Adamawa State) recorded the highest precipitation in August with value of 255.2 mm. It is observed that Abeokuta (in Ogun State), Ibadan (Oyo State) and Ikeja (in Lagos State) experienced rainfall throughout the entire period.

The Southwest experience low rainfall during the dry season (November–March) while the wet season (April–October) expectedly recorded higher amount of rainfall. Abeokuta (in Ogun State) had the highest average rainfall of 264 mm in August while Ibadan (Oyo State) and Ikeja (in Lagos State) recorded the highest amount of rainfall in the months of September and June with the values of 205.2 mm and 280.1 mm respectively.

These months of observed peak rainfall are indicative of worst months of a radio link in the various locations (Ojo and Olurotimi, 2014). Also, the observed seasonal rainfall variation is attributed to the prevailing weather conditions in the area under study: During the dry season, the entire country is under the influence of dry continental air because of the dry and cold North Easterly tropical continental (cT) air mass over the region (often accompanied by dust particles transported from the Sahara desert),which coincides with a period of minimum or no rain. In the wet season period, the deep moist maritime air predominates along with the characteristic heavy rainfall from the South-Westerly, tropical maritime (mT) air mass bringing moisture on to the country from the Southern hemisphere (Ojo,1977). The stations characteristics including the average annual rainfall for 33years and yearly total rainfall are given in appendix A and B respectively.

4.3 Rain Rate calculation for the locations using Chebil Model

The point rainfall values calculated for the study areas was obtained using Chebil model. The point rainfall rate exceeded for 0.01% of an average year is given in Table 4.1

Table 4.1: Point rainfall rate for the study area

Locations	Yola	Gombe	Jalingo	Abeokuta	Ibadan	Ikeja
$R_{0.01}$ **(mm/h)**	90.34	94.4	96.2	99.7	104.8	108.2

The results from Table 4.1 show that higher rainfall rate at 0.01% exceedance was recorded in Ikeja, Ibadan and Abeokuta than in Yola, Gombe and Jalingo at the same time exceedance percentage. Hence, higher rain attenuation is expected in the Southwest region than in the Northeast region.

The geographical and experimental parameters used for the Northeast Stations is presented in Table 4.2

Table 4.2: Geographical and experimental parameters for the Northeast Stations.

Location	Yola	Gombe	Jalingo
Longitude	12.27°	11.02°	11.30°
Latitude	9.13°	10.19°	8.54°
Elevation angle	23°, 42.5° and 55°	23°, 42.5° and 55°	23°, 42.5° and 55°
Isotherm height (km)	4.41	4.42	4.38
Polarisation	horizontal,vertical and circular	horizontal,vertical and circular	horizontal,vertical and circular
Operational frequencies	downlink (11GHz) and uplink(14GHz) for Ku-band, downlink (20GHz) and uplink(40GHz) for Ka-band,	downlink (11GHz) and uplink(14GHz) for Ku-band, downlink (20GHz) and uplink(40GHz) for Ka-band,	downlink (11GHz) and uplink(14GHz) for Ku-band, downlink (20GHz) and uplink(40GHz) for Ka-band,

The geographical and experimental parameters used for the Southwest Stations is presented in Table 4.3

Table 4.3: Geographical and experimental parameters for the Southwest Stations.

Location	Abeokuta	Ibadan	Ikeja
Longitude	3.55°	3.9°	3.33°
Latitude	6.42°	7.43°	6.58°
Elevation angle	23°, 42.5° and 55°	23°, 42.5° and 55°	23°, 42.5° and 55°
Isotherm height (km)	4.41	4.4	4.38
Polarisation	horizontal,vertical and circular	horizontal,vertical and circular	horizontal,vertical and circular
Operational frequencies	downlink (11GHz) and uplink(14GHz) for Ku-band, downlink (20GHz) and uplink(40GHz) for Ka-band,	downlink (11GHz) and uplink(14GHz) for Ku-band, downlink (20GHz) and uplink(40GHz) for Ka-band,	downlink (11GHz) and uplink(14GHz) for Ku-band, downlink (20GHz) and uplink(40GHz) for Ka-band,

The specific attenuation for horizontal polarisation of the study area (dB/km) shown in Table 4.4

Table 4.4: Specific attenuation for horizontal polarisation of the study area (dB/km)

Frequency (GHz)	Yola	Gombe	Jalingo	Abeokuta	Ibadan	Ikeja
11.00	4.20	4.43	4.53	4.39	5.03	5.22
14.00	6.33	6.66	6.80	6.60	7.50	7.78
20.00	10.69	11.20	11.43	11.11	12.51	12.94
40.00	22.02	22.88	23.25	22.73	25.05	25.75

The specific attenuation for vertical polarisation of the study area (dB/km) shown in Table 4.5

Table 4.5: Specific attenuation for vertical polarisation of the study area (dB/km)

Frequency (GHz)	Yola	Gombe	Jalingo	Abeokuta	Ibadan	Ikeja
11.00	3.24	3.41	3.48	3.38	3.85	3.99
14.00	4.99	5.22	5.33	5.18	5.84	6.04
20.00	8.10	8.46	8.62	8.40	9.38	9.68
40.00	18.96	19.68	19.99	19.55	21.49	22.07

The specific attenuation for circular polarisation of the study area (dB/km) shown in Table 4.6

Table 4.6: Specific attenuation for circular polarisation of the study area (dB/km)

Frequency (GHz)	Yola	Gombe	Jalingo	Abeokuta	Ibadan	Ikeja
11.00	3.69	3.89	3.98	3.86	4.40	4.57
14.00	5.58	5.86	5.98	5.81	6.57	6.80
20.00	9.28	9.70	9.89	9.63	10.79	11.15
40.00	20.46	21.24	21.59	21.11	23.23	23.87

The horizontal reduction factor for horizontal polarisation of the study area (dB/km) shown in Table 4.7

Table 4.7: Horizontal reduction factor for horizontal polarisation of the study area (dB/km)

Frequency (GHz)	Yola	Gombe	Jalingo	Abeokuta	Ibadan	Ikeja
11.00	0.67	0.67	0.67	0.66	0.64	0.63
14.00	0.64	0.64	0.63	0.63	0.61	0.60
20.00	0.61	0.61	0.60	0.60	0.58	0.57
40.00	0.60	0.61	0.60	0.59	0.58	0.57

The horizontal reduction factor for vertical Polarisation of the study area (dB/km) shown in Table 4.8

Table 4.8: Horizontal reduction factor for vertical Polarisation of the study area (dB/km)

Frequency (GHz)	Yola	Gombe	Jalingo	Abeokuta	Ibadan	Ikeja
11.00	0.73	0.72	0.72	0.71	0.69	0.68

14.00	0.69	0.69	0.68	0.68	0.65	0.64
20.00	0.66	0.66	0.66	0.65	0.63	0.62
40.00	0.63	0.63	0.63	0.62	0.61	0.60

The horizontal reduction factor for circular polarisation of the study area (dB/km) shown in Table 4.9

Table 4.9: Horizontal reduction factor for circular polarisation of the study Area (dB/km)

Frequency (GHz)	Yola	Gombe	Jalingo	Abeokuta	Ibadan	Ikeja
11.00	0.70	0.70	0.69	0.69	0.66	0.65
14.00	0.67	0.67	0.66	0.65	0.63	0.62
20.00	0.64	0.64	0.63	0.62	0.61	0.60
40.00	0.62	0.62	0.61	0.61	0.59	0.58

The path length for horizontal polarisation of the study area (dB/km) shown in Table 4.10

Table 4.10: Path length for horizontal polarisation of the study area (dB/km)

Frequency (GHz)	Yola	Gombe	Jalingo	Abeokuta	Ibadan	Ikeja
11.00	3.98	3.80	3.81	4.01	3.80	3.80
14.00	3.77	3.60	3.62	3.79	3.60	3.60
20.00	3.57	3.41	3.42	3.59	3.41	3.41
40.00	3.53	3.38	3.40	3.56	3.41	3.42

The path length for vertical polarisation of the study area (dB/km) shown in Table 4.11

Table 4.11: Path length for vertical polarisation of the study area (dB/km)

Frequency (GHz)	Yola	Gombe	Jalingo	Abeokuta	Ibadan	Ikeja
11.00	4.32	4.12	4.14	4.35	4.13	4.14
14.00	4.07	3.89	3.91	4.10	3.91	3.91
20.00	3.91	3.74	3.76	3.94	3.76	3.77
40.00	3.71	3.56	3.58	3.75	3.60	3.61

The Path length for circular polarisation of the study area (dB/km) shown in Table 4.12

Table 4.12: Path length for circular polarisation of the study area (dB/km)

Frequency (GHz)	Yola	Gombe	Jalingo	Abeokuta	Ibadan	Ikeja
11.00	4.15	3.95	3.97	4.17	3.96	3.96
14.00	3.93	3.75	3.77	3.96	3.76	3.76
20.00	3.74	3.57	3.59	3.77	3.59	3.59
40.00	3.62	3.47	3.49	3.65	3.50	3.51

The vertical adjustment factor for horizontal polarisation of the study area (dB/km) shown in Table 4.13

Table 4:13: Vertical adjustment factor for horizontal polarisation of the study area (dB/km)

Frequency (GHz)	Yola	Gombe	Jalingo	Abeokuta	Ibadan	Ikeja
11.00	0.81	0.81	0.84	0.83	0.82	0.81
14.00	0.95	0.95	0.98	0.97	0.96	0.95
20.00	1.16	1.16	1.19	1.18	1.17	1.16
40.00	1.51	1.51	1.53	1.53	1.52	1.52

The vertical adjustment factor for vertical polarisation of the study area (dB/km) shown in Table 4.14

Table 4:14: Vertical adjustment factor for vertical polarisation of the study area (dB/km)

Frequency (GHz)	Yola	Gombe	Jalingo	Abeokuta	Ibadan	Ikeja
11.00	0.81	0.81	0.84	0.83	0.82	0.81
14.00	0.95	0.95	0.98	0.97	0.96	0.95
20.00	1.16	1.16	1.19	1.18	1.17	1.16
40.00	1.51	1.51	1.53	1.53	1.52	1.52

The vertical adjustment factor for circular polarisation of the study area (dB/km) shown in Table 4.15

Table 4:15: Vertical adjustment factor for circular polarisation of the study area (dB/km)

Frequency (GHz)	Yola	Gombe	Jalingo	Abeokuta	Ibadan	Ikeja
11.00	0.83	0.83	0.86	0.85	0.84	0.83
14.00	0.97	0.97	1.00	0.99	0.98	0.97
20.00	1.18	1.18	1.21	1.20	1.19	1.18
40.00	1.52	1.52	1.53	1.53	1.53	1.52

The effective path length for horizontal polarisation of the study area (dB/km) shown in Table 4.16

Table 4:16: Effective path length for horizontal polarisation of the study area (dB/km)

Frequency (GHz)	Yola	Gombe	Jalingo	Abeokuta	Ibadan	Ikeja
11.00	3.23	3.07	3.20	3.34	3.10	3.07
14.00	3.57	3.41	3.53	3.69	3.44	3.42
20.00	4.14	3.95	4.06	4.24	3.99	3.96
40.00	5.34	5.12	5.20	5.44	5.18	5.18

The effective path length for vertical polarisation of the study area (dB/km) shown in Table 4.17

Table 4:17: Effective path length for vertical polarisation of the study area (dB/km)

Frequency (GHz)	Yola	Gombe	Jalingo	Abeokuta	Ibadan	Ikeja
11.00	3.67	3.50	3.64	3.80	3.54	3.51
14.00	4.01	3.83	3.96	4.14	3.88	3.86
20.00	4.68	4.48	4.60	4.81	4.54	4.53

40.00	5.66	5.42	5.52	5.76	5.51	5.51

The effective path length for circular polarisation of the study area (dB/km) shown in Table 4.18

Table 4.18: Effective path length for circular polarisation of the study area (dB/km)

Frequency (GHz)	Yola	Gombe	Jalingo	Abeokuta	Ibadan	Ikeja
11.00	3.44	3.28	3.41	3.56	3.31	3.28
14.00	3.80	3.63	3.76	3.92	3.67	3.64
20.00	4.41	4.21	4.33	4.53	4.27	4.25
40.00	5.50	5.27	5.36	5.60	5.34	5.34

The results of the effective path lengths at 0.01% unavailability shows that the slant path length, L_S and the horizontal projection length, L_G were longest in Abeokuta followed by Yola, Jalingo, Ibadan,Ikeja and Gombe . The reason for Abeokuta L_S and L_G being the longest and Gombe`s L_S and L_G being the lowest could be due to their geometrical height above the mean sea level. Also, the effective path lengths through rain increases with increasing frequency for all the locations. From the results of rain attenuation, it is seen that when the attenuation is increased the time duration will decrease in all the locations. This is

due to the heavy rains which cause high attenuation levels at short duration. It is because the higher attenuation depends on large rain drop size and high rain intensity.

The predicted attenuation exceeded at 0.01% of an average year at different operating frequencies and polarisations are shown in appendix C.

Attenuation varies from location to location due to different rainfall rate experienced in various locations. Ikeja, Ibadan and Abeokuta recorded higher rainfall rate when compared to other stations hence there is more signal attenuation occurrence. Rain does not occur all the time in the year and its rate does not remain the same all the time when it occurs, therefore the amount of rain fade margin needed to compensate for the rain effect varies with time.

In Yola, for horizontal polarisation, the attenuation was 13.55 dB at 11GHz and 22.64 dB at 14 GHz for Ku-band, 44.22 dB at 20 GHz and 117.59 dB at 40 GHz for Ka-band. For vertical polarisation, the attenuation was 11.89 dB at 11GHz and 19.99 dB at 14 GHz for Ku-band, 37.93 dB at 20 GHz and 107.32 dB at 40 GHz for Ka-band. For circular polarisation, attenuation was 12.71 dB at 11GHz and 21.20 dB at 14 GHz for Ku-band, 40.90 dB at 20 GHz and 112.44 dB at 40 GHz for Ka-band. In Gombe, for horizontal polarisation, the attenuation was 1.36 dB at 11GHz and 22.68 dB at 14 GHz for Ku-band, 44.23 dB at 20 GHz and 117.03 dB at 40 GHz for Ka-band. For vertical polarisation attenuation was 11.92 dB at 11GHz and 19.99 dB at 14 GHz for Ku-band, 37.88 dB at 20 GHz and 106.73 dB at 40 GHz for Ka-band. For circular polarisation, the attenuation was 12.75 dB at 11GHz and 21.23 dB at 14 GHz for Ku-band, 40.88 dB at 20 GHz and 111.86 dB at 40 GHz for Ka-band. In Jalingo, for horizontal polarisation, the attenuation was 14.48 dB at 11GHz and 24.02 dB at 14 GHz for Ku-band, 46.43 dB at 20

GHz and 121.03 dB at 40 GHz for Ka-band. For vertical polarisation, attenuation was 12.68 dB at 11GHz and 21.14 dB at 14 GHz for Ku-band, 39.6896 dB at 20 GHz and 110.32 dB at 40 GHz for the Ka-band. For circular polarisation, the attenuation was 13.57 dB at 11GHz and 22.46 dB at 14 GHz for the Ku-band, 42.87 dB at 20 GHz and 115.66 dB at 40 GHz for Ka-band. In Abeokuta, for horizontal polarisation attenuation was 14.66 dB at 11GHz and 24.02 dB at 14 GHz for Ku-band, 46.43 dB at 20 GHz and 123.57 dB at 40 GHz for Ka-band. For vertical polarisation, attenuation was 12.85 dB at 11GHz and 21.47 dB at 14 GHz for Ku-band, 40.39 dB at 20 GHz and 112.71 dB at 40 GHz for Ka-band. For circular polarisation attenuation was 13.74 dB at 11GHz and 22.79 dB at 14 GHz for Ku-band, 43.59 dB at 20 GHz and 118.12 dB at 40 GHz for Ka-band. In Ibadan, for horizontal polarisation, attenuation was 15.55 dB at 11GHz and 25.78 dB at 14 GHz for Ku-band, 49.88 dB at 20 GHz and 129.84 dB at 40 GHz for Ka-band. For vertical polarisation, attenuation was 13.6278 dB at 11GHz and 22.68 dB at 14 GHz for Ku-band, 42.61 dB at 20 GHz and 118.33dB at 40 GHz for Ka-band. For circular polarisation attenuation was 14.58 dB at 11GHz and 24.11 dB at 14 GHz for Ku-band, 46.04 dB at 20 GHz and 124.06 dB at 40 GHz for Ka-band.In Ikeja, for horizontal polarisation attenuation was 15.95 dB at 11GHz and 26.44 dB at 14 GHz for Ku-band, 51.29 dB at 20 GHz and 133.48 dB at 40 GHz for Ka-band. For vertical polarisation attenuation was 14.01 dB at 11GHz and 23.31 dB at 14 GHz for Ku-band, 43.81 dB at 20 GHz and 121.64 dB at 40 GHz for Ka-band.For circular polarisation attenuation was 14.99 dB at 11GHz and 23.31 dB at 14 GHz for Ku-band, 47.34 dB at 20 GHz and 127.54 dB at 40 GHz for Ka-band.

Figure 4.2-4.37 shows the result of the rain attenuation for horizontally, vertically and circularly polarised signal experienced for different percentages of time using ITU-R

P.618-12 model and for Ku-band (11 GHz and 14 GHz) and Ka-band (20 GHz and 40 GHz) respectively. For 0.01% of the year (i.e 99.99%) using horizontal polarisation, the rain attenuation in Yola at Ku-band are 13.55 dB and 22.64 dB respectively. At Ka-band are 44.22 dB and 117.59 dB respectively. Similarly in Gombe the rain attenuation for Ku-band are 13.36 dB and 22.68 dB respectively. At Ka-band are 44.23 dB and 117.03 dB respectively. In Jalingo the rain attenuation for Ku-band frequency are 14.48 dB and 24.02 dB respectively. At Ka-band frequency are 46.43 dB and 121.03 dB respectively. In Abeokuta the rain attenuation for Ku-band are 14.66 dB and 24.02 dB respectively. At Ka-band are 46.43 dB and 123.57 dB respectively. In Ibadan the rain attenuation for Ku-band frequency are 15.55 dB and 25.78 dB respectively. At Ka-band frequency are 49.88 dB and 129.84 dB respectively. In Ikeja the rain attenuation for Ku-band frequency are 15.95 dB and 26.44 dB respectively. At Ka-band frequency are 51.29 dB and 133.48dB respectively. This shows that attenuation experienced in Yola, Gombe and Jalingo is less compared to that experienced in Abeokuta ,Ibadan and Ikeja. From the results obtained in figure 4.37, increase in frequency leads to corresponding increase in attenuation, attenuation is also said to be function of frequency which is also true from the results. The estimated attenuation to be exceeded for other percentages of an average year, in the range 0.001% to 10%, is determined from the attenuation to be exceeded for 0.01% for an average year. This method provides an estimate of the long-term statistics of attenuation due to rain.

Figures 4.2 – 4.13 show the graphical comparison of the rain attenuation in the study area for horizontal, vertical and circulation polarisations of 42.5° elevation angle at different percentage of time.

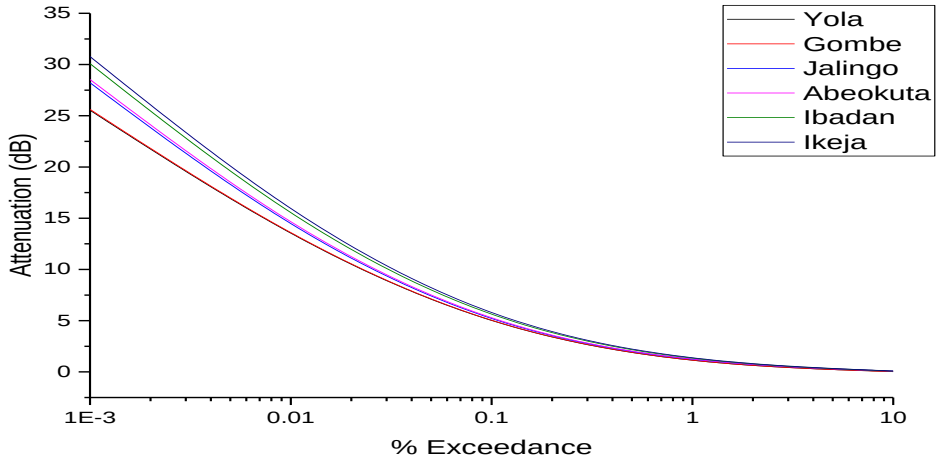

Figure 4.2: Rain attenuation at 11GHz and 42.5° for horizontal polarisation

From Figure 4.2, the rain attenuation at Ku-band downlink frequency for Yola, Gombe, Jalingo, Abeokuta, Ibadan and Ikeja at 0.01% time exceedance was observed to be 13.54 dB, 13.59 dB, 14.48 dB, 14.66 dB, 15.55 dB and 15.95 dB respectively.

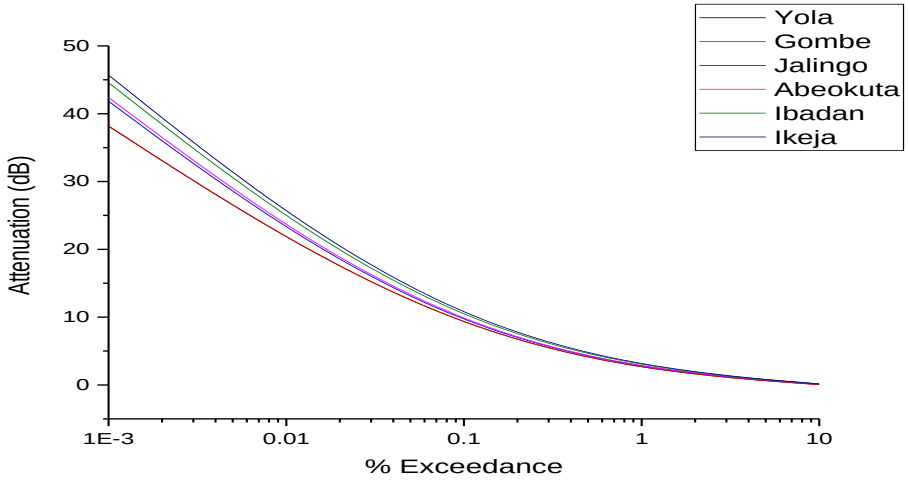

Figure 4.3: Rain attenuation at 14 GHz and 42.5° elevation angle for horizontal polarisation

From Figure 4.3, the rain attenuation computed at Ku-band uplink frequency for Yola, Gombe, Jalingo, Abeokuta, Ibadan and Ikeja at 0.01% time exceedance was 22.64 dB, 22.68 dB, 24.02 dB, 24.35 dB, 25.78dB and 26.44 dB respectively.

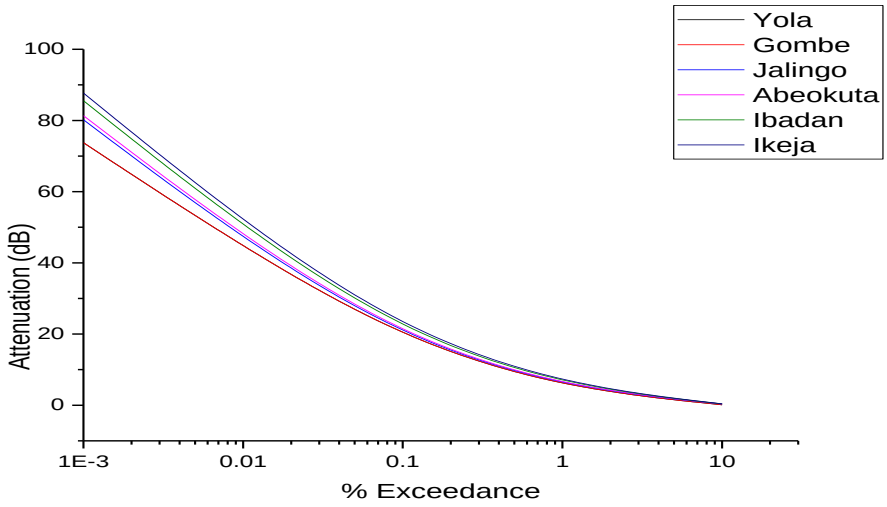

Figure 4.4: Rain attenuation at 20 GHz and 42.5° elevation angle for horizontal polarisation

From Figure 4.4, the rain attenuation at Ka-band downlink frequency for Yola, Gombe, Jalingo, Abeokuta, Ibadan and Ikeja at 0.01% time exceedance was observed to be 44.22 dB, 44.23 dB, 46.43 dB, 47.17 dB, 49.88 dB and 51.30 dB respectively.

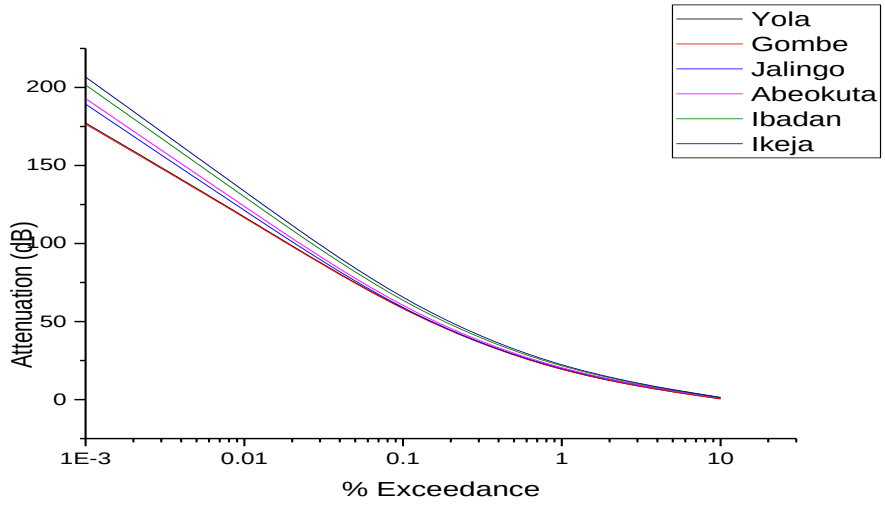

Figure 4.5: Rain attenuation at 40 GHz and 42.5° elevation angle for horizontal polarisation

From Figure 4.5, the rain attenuation computed at Ka-band downlink frequency for Yola, Gombe, Jalingo, Abeokuta, Ibadan and Ikeja at 0.01% time exceedance was 117.59 dB, 117.03 dB, 121.03 dB, 123.57 dB, 129.84 dB and 133.48 dB respectively.

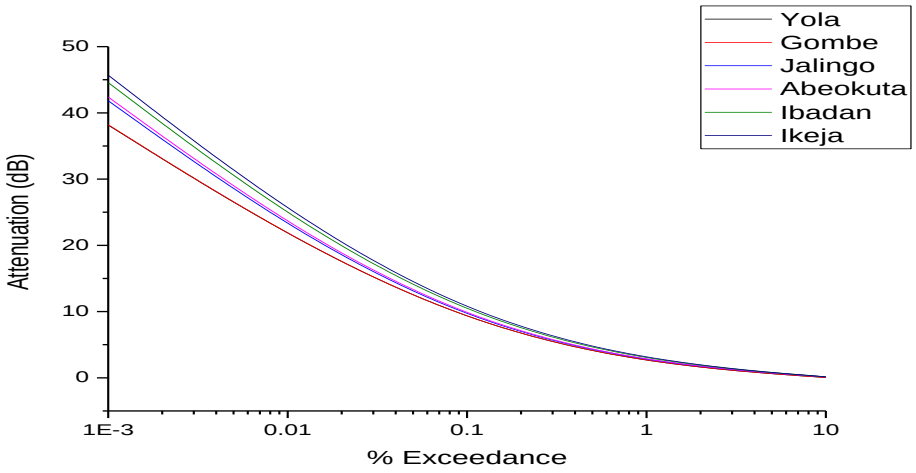

Figure 4.6: Rain attenuation at 11 GHz and 42.5° elevation angle for vertical polarisation

From Figure 4.6, the rain attenuation at Ku-band downlink frequency for Yola, Gombe, Jalingo, Abeokuta, Ibadan and Ikeja at 0.01% time exceedance was observed to be 44.22 dB, 44.23 dB, 46.43 dB, 47.17 dB, 49.88 dB and 51.30 dB respectively

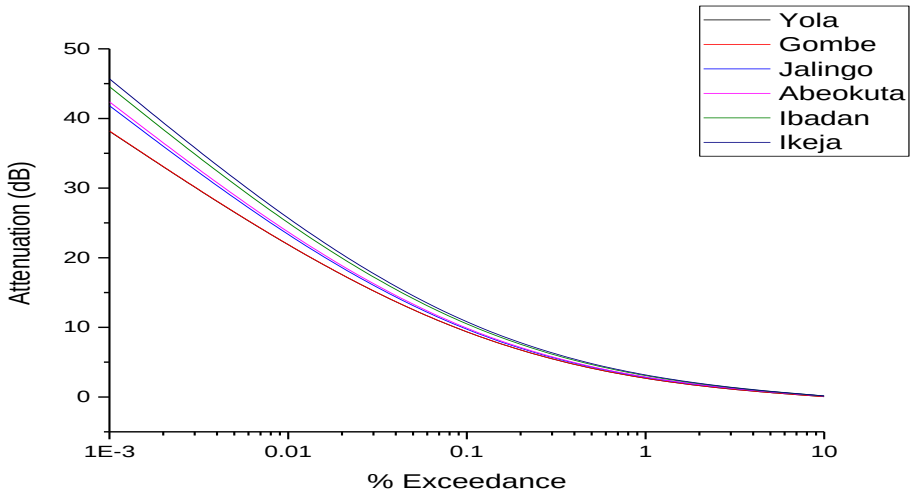

Figure 4.7: Rain attenuation at 14 GHz and 42.5° elevation angle for vertical polarisation

From Figure 4.7, the rain attenuation computed at Ku-band uplink frequency for Yola, Gombe, Jalingo, Abeokuta, Ibadan and Ikeja at 0.01% time exceedance was 19.99 dB, 19.99 dB, 21.12 dB, 21.47 dB, 22.68 dB and 23.31 dB respectively.

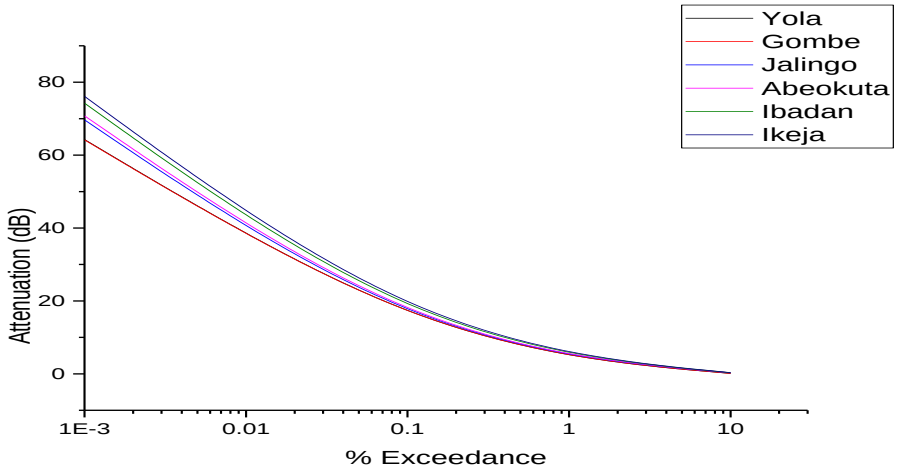

Figure 4.8: Rain attenuation at 20 GHz and 42.5° elevation angle for vertical polarisation

From Figure 4.8, the rain attenuation at Ka-band downlink frequency for Yola, Gombe, Jalingo, Abeokuta, Ibadan and Ikeja at 0.01% time exceedance was observed to be 37.93 dB, 37.88 dB, 39.69 dB, 40.39dB,42.61 dB and 43.81 dB respectively.

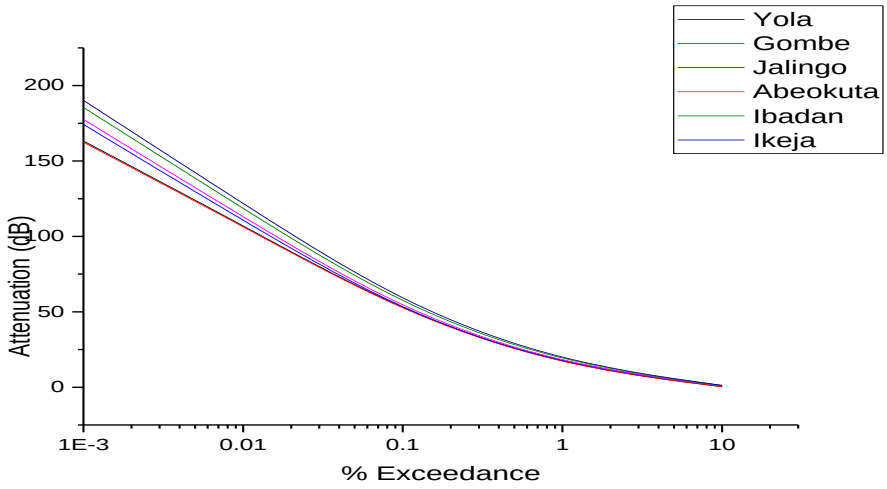

Figure 4.9: Rain attenuation at 40 GHz and 42.5° elevation angle for vertical polarisation

From Figure 4.9, the rain attenuation computed at Ka-band uplink frequency for Yola, Gombe, Jalingo, Abeokuta, Ibadan and Ikeja at 0.01% time exceedance was 107.32 dB, 106.73 dB, 110.32 dB,112.71 dB, 118.33 dB and 121.64 dB respectively.

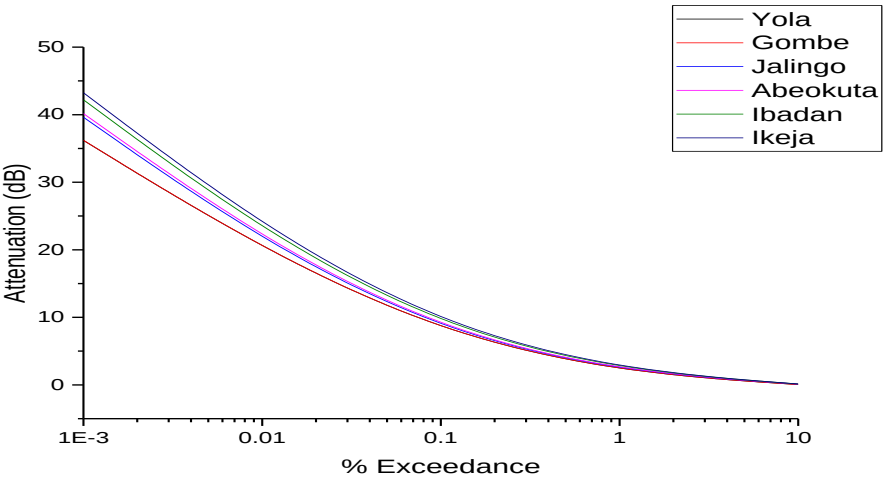

Figure 4.10: Rain attenuation at 11 GHz and 42.5° elevation angle for circular polarisation

From Figure 4.10, the rain attenuation at Ku-band downlink frequency for Yola, Gombe, Jalingo, Abeokuta, Ibadan and Ikeja at 0.01% time exceedance was observed to be 12.71 dB, 12.75 dB,13.57 dB, 13.74 dB, 14.58 dB and 14.99 dB respectively.

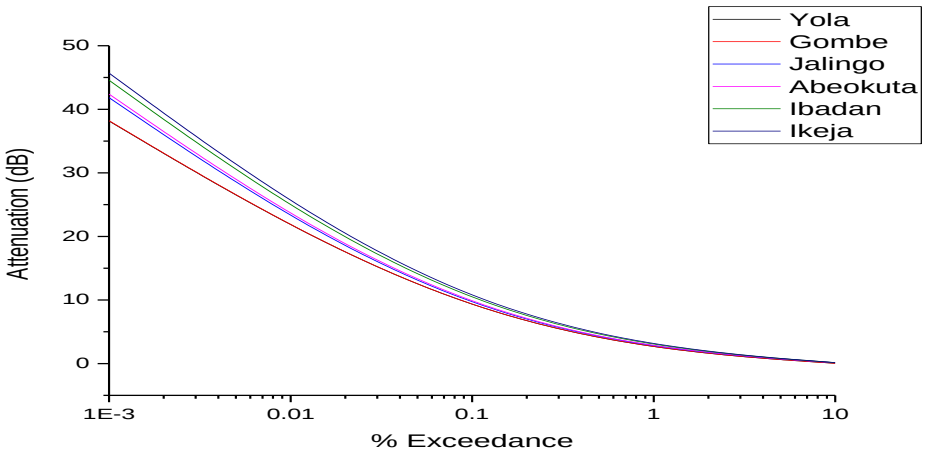

Figure 4.11: Rain attenuation at 14 GHz and 42.5° elevation angle for circular polarisation

From Figure 4.11, the rain attenuation computed at Ku-band downlink frequency for Yola, Gombe, Jalingo, Abeokuta, Ibadan and Ikeja at 0.01% time exceedance was 21.20 dB, 21.23 dB, 22.46 dB, 22.79 dB, 24.11 dB and 24.78 dB respectively.

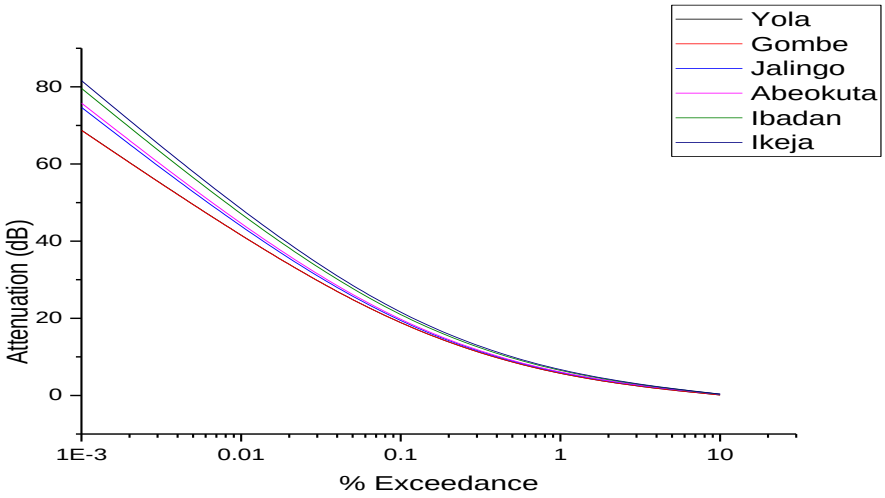

Figure 4.12: Rain attenuation at 20 GHz and 42.5° elevation angle for circular polarisation

From Figure 4.12, the rain attenuation at Ka-band uplink frequency for Yola, Gombe, Jalingo, Abeokuta, Ibadan and Ikeja at 0.01% time exceedance was observed to be 40.90 dB, 40.88 dB, 42.87 dB, 43.59 dB,46.04 dB and 47.34 dB respectively.

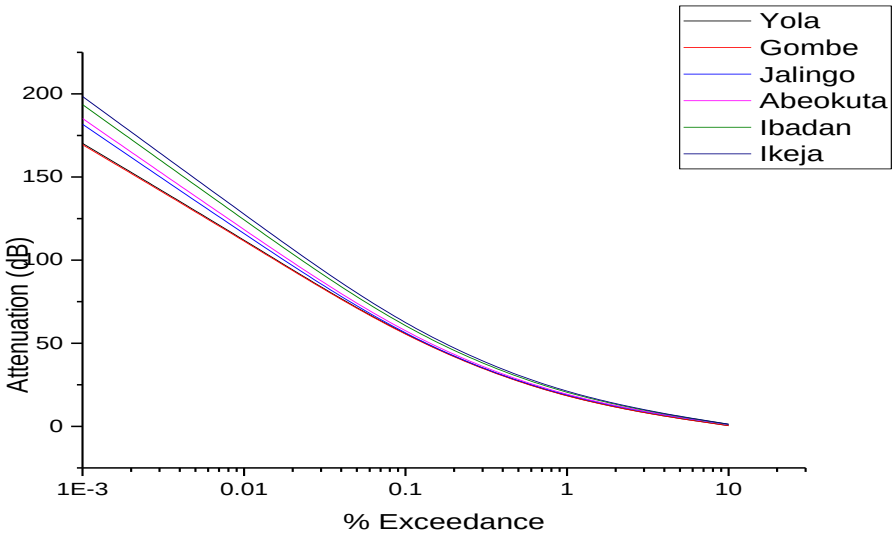

Figure 4.13: Rain attenuation at 40 GHz and 42.5° elevation angle for circular polarisation

From Figure 4.13, the rain attenuation at Ka-band uplink frequency for Yola, Gombe, Jalingo, Abeokuta, Ibadan and Ikeja at 0.01% time exceedance was observed to be 112.44 dB,111.86 dB, 115.66 dB, 118.12 dB, 124.06 dB and 127.54 dB respectively.

Figure 4.14 – 4.25 Shows the graphical comparison of the rain attenuation in the study area for horizontal, vertical and circular polarisation of 55° elevation angle at different percentage of time.

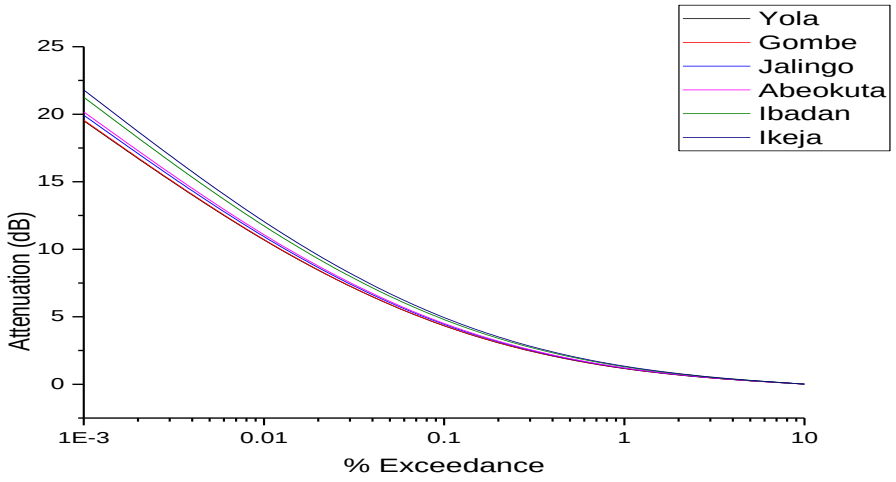

Figure 4.14: Rain attenuation at 11 GHz and 55° elevation angle for horizontal polarisation.

From Figure 4.14 , the rain attenuation at Ku-band downlink frequency for Yola, Gombe, Jalingo, Abeokuta, Ibadan and Ikeja at 0.01% time exceedance was observed to be 11.66 dB, 11.71 dB, 11.94 dB, 12.09 dB, 12.83 dB and 13.19 dB respectively.

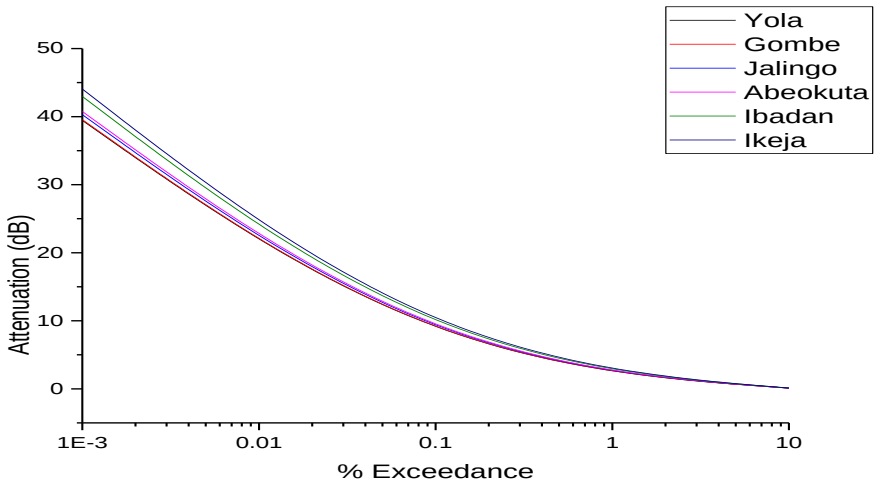

Figure 4.15: Rain attenuation at 14 GHz and 55° elevation angle for horizontal polarisation

From Figure 4.15, the rain attenuation computed at Ku-band downlink frequency for Yola, Gombe, Jalingo, Abeokuta, Ibadan and Ikeja at 0.01% time exceedance was 19.79 dB, 19.84 dB, 20.24 dB, 20.53 dB, 21.73 dB and 22.34 dB respectively.

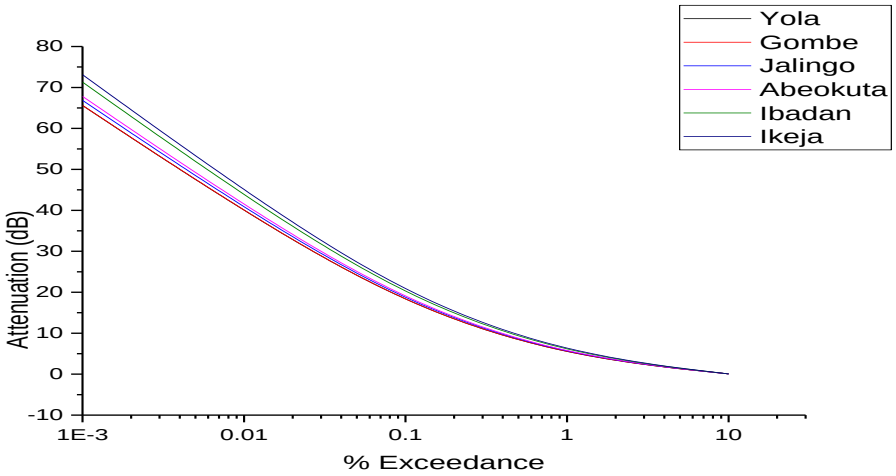

Figure 4.16: Rain attenuation at 20 GHz and 55° elevation angle for horizontal polarisation

From Figure 4.16, the rain attenuation at Ku-band downlink frequency for Yola, Gombe, Jalingo, Abeokuta, Ibadan and Ikeja at 0.01% time exceedance was observed to be 39.54 dB, 39.55 dB, 40.38 dB, 41.03 dB, 43.40 dB and 44.63 dB respectively.

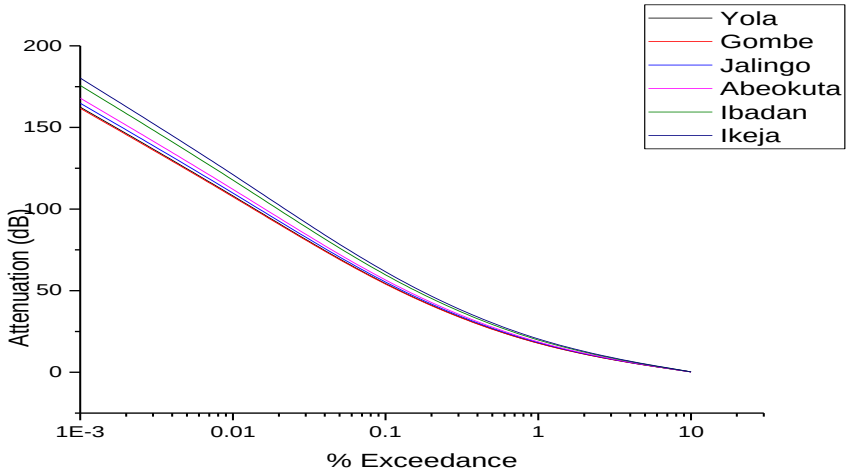

Figure 4.17: Rain attenuation at 40 GHz and 55° elevation angle for horizontal polarisation

From Figure 4.17, the rain attenuation computed at Ku-band downlink frequency for Yola, Gombe, Jalingo, Abeokuta, Ibadan and Ikeja at 0.01% time exceedance was 108.74 dB, 108.20 dB, 110.52 dB, 112.89 dB, 118.72 dB and 122.11 dB respectively.

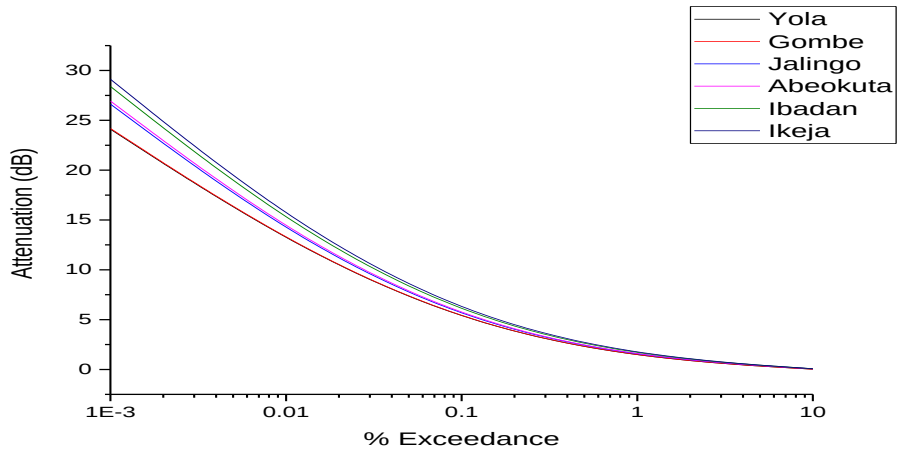

Figure 4.18: Rain attenuation at 11 GHz and 55° elevation angle for vertical polarisation

From Figure 4.18, the rain attenuation at Ku-band downlink frequency for Yola, Gombe, Jalingo, Abeokuta, Ibadan and Ikeja at 0.01% time exceedance was observed to be 10.22 dB, 10.25 dB, 10.46 dB, 10.61 dB, 11.25 dB and 11.56 dB respectively.

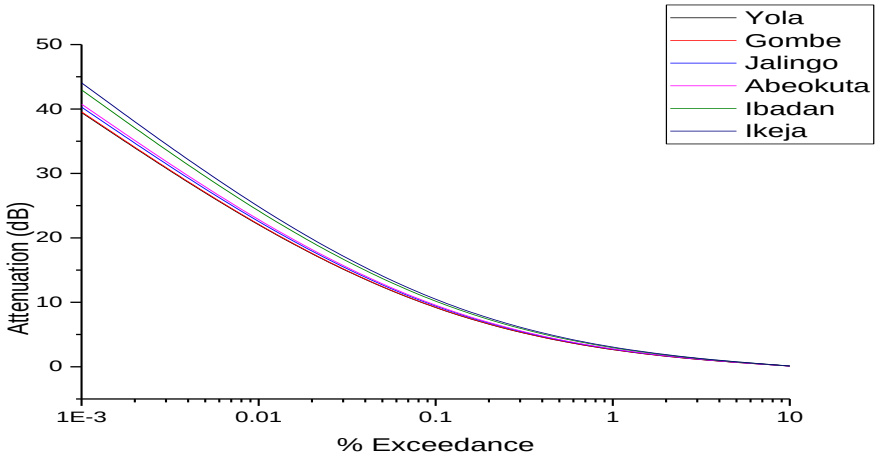

Figure 4.19: Rain attenuation at 14 GHz and 55° elevation angle for vertical polarisation

From Figure 4.19 , the rain attenuation at Ku-band downlink frequency for Yola, Gombe, Jalingo, Abeokuta, Ibadan and Ikeja at 0.01% time exceedance was observed to be 17.45 dB, 17.46 dB, 17.82dB, 18.09 dB, 19.11 dB and 19.64 dB respectively.

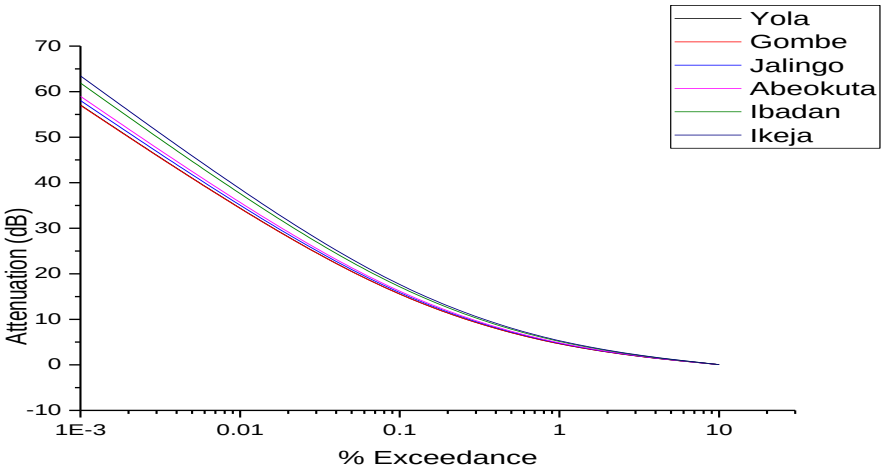

Figure 4.20: Rain attenuation at 20 GHz and 55° elevation angle for vertical polarisation

From Figure 4.20, the rain attenuation computed at Ku-band downlink frequency for Yola, Gombe, Jalingo, Abeokuta, Ibadan and Ikeja at 0.01% time exceedance was 33.85 dB, 33.79 dB, 34.50 dB, 35.12 dB, 37.05 dB and 38.10 dB respectively.

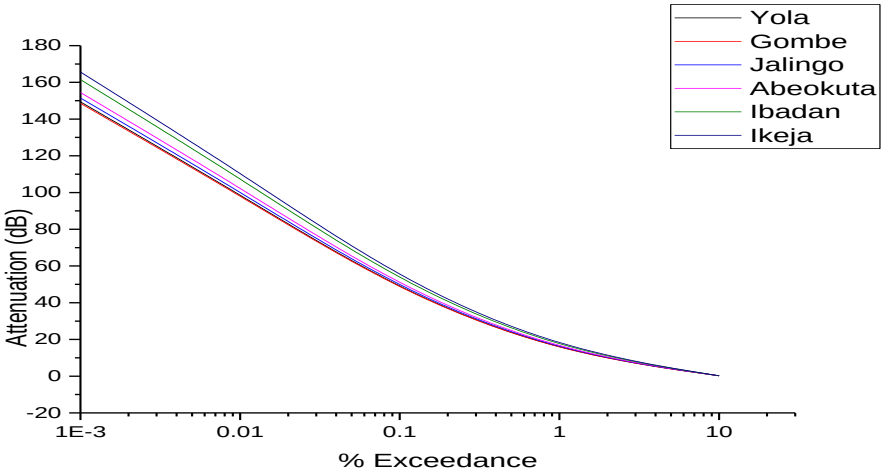

Figure 4.21: Rain attenuation at 40 GHz and 55° elevation angle for vertical polarisation

From Figure 4.21, the rain attenuation at Ku-band downlink frequency for Yola, Gombe, Jalingo, Abeokuta, Ibadan and Ikeja at 0.01% time exceedance was observed to be 99.01 dB, 98.44 dB, 100.56dB, 102.80 dB, 108.01 dB and 111.10 dB respectively.

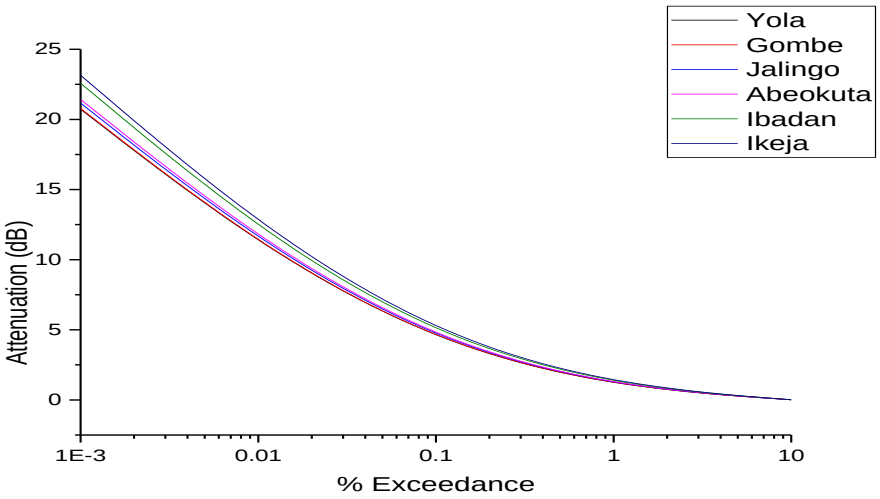

Figure 4.22: Rain attenuation at 11 GHz and 55° elevation angle for cirular polarisation

From Figure 4.22, the rain attenuation computed at Ku-band downlink frequency for Yola, Gombe, Jalingo, Abeokuta, Ibadan and Ikeja at 0.01% time exceedance was 10.94 dB, 10.97 dB, 11.19 dB, 11.34 dB, 12.03 dB and 12.37 dB respectively.

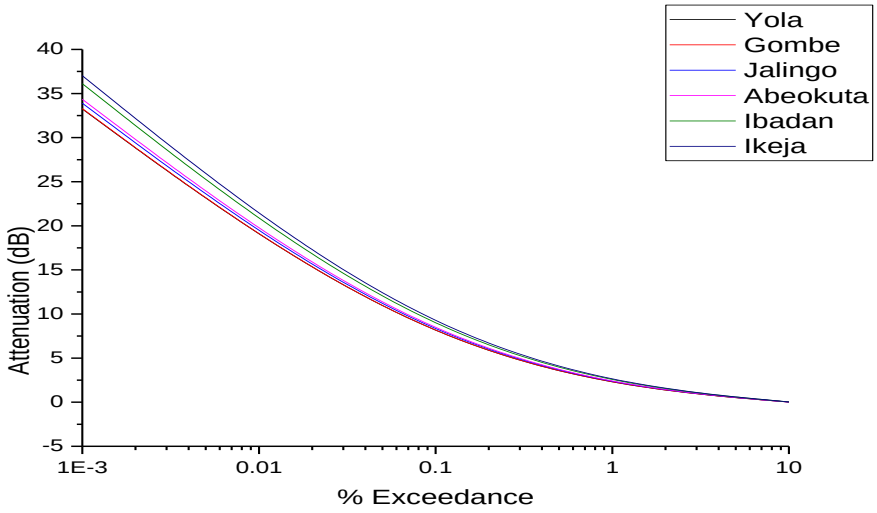

Figure 4.23: Rain attenuation at 14 GHz and 55° elevation angle for circular polarisation

From Figure 4.23, the rain attenuation at Ku-band downlink frequency for Yola, Gombe, Jalingo, Abeokuta, Ibadan and Ikeja at 0.01% time exceedance was observed to be 18.53 dB, 18.55 dB, 18.93 dB, 19.21 dB, 20.32 dB and 20.88 dB respectively

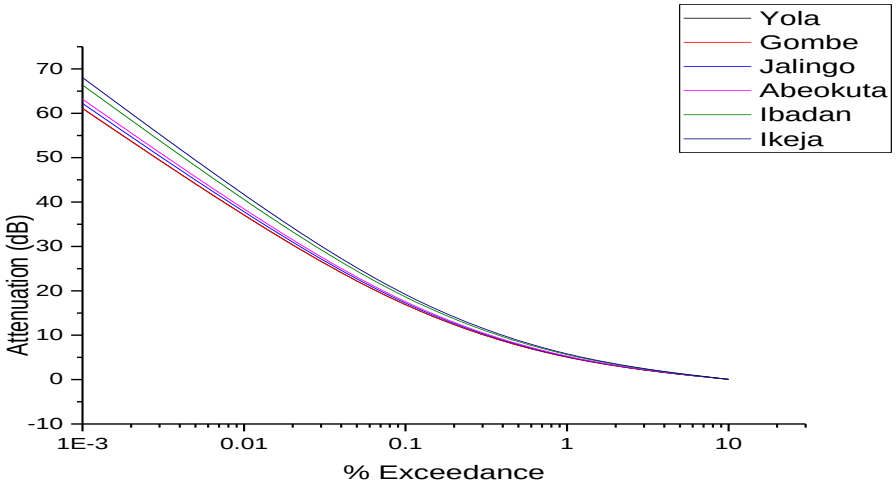

Figure 4.24: Rain attenuation at 20 GHz and 55° elevation angle for circular polarisation

From Figure 4.24, the rain attenuation at Ku-band downlink frequency for Yola, Gombe, Jalingo, Abeokuta, Ibadan and Ikeja at 0.01% time exceedance was observed to be 36.54 dB, 36.51 dB, 37.28 dB, 37.91 dB, 40.05 dB and 41.18 dB respectively.

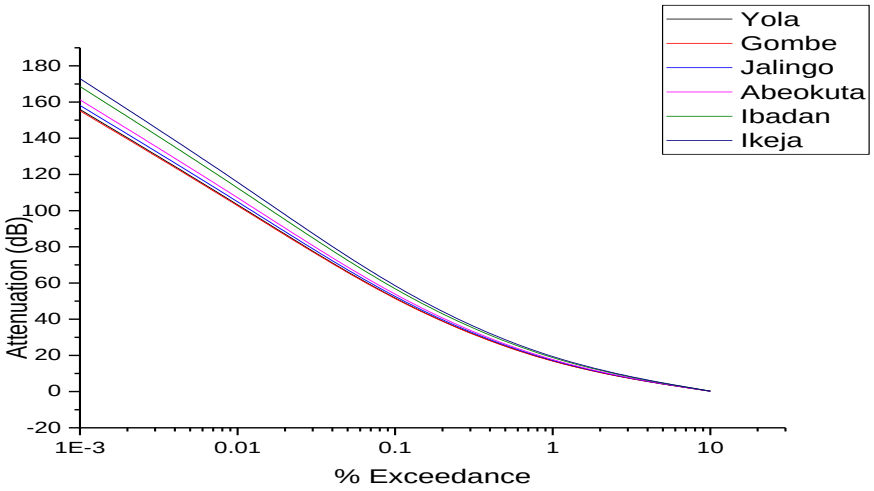

Figure 4.25: Rain attenuation at 40 GHz and 55° elevation angle for circular polarisation

From Figure 4.25, the rain attenuation computed at Ku-band downlink frequency for Yola, Gombe, Jalingo, Abeokuta, Ibadan and Ikeja at 0.01% time exceedance was 103.86 dB, 103.30 dB, 105.52 dB, 107.83 dB, 113.35 dB and 116.58 dB respectively.

Figure 4.26 – 4.37 shows the graphical comparison of the rain attenuation in the study area for horizontal, vertical and circular polarisations of 23° elevation angle at different percentage of time

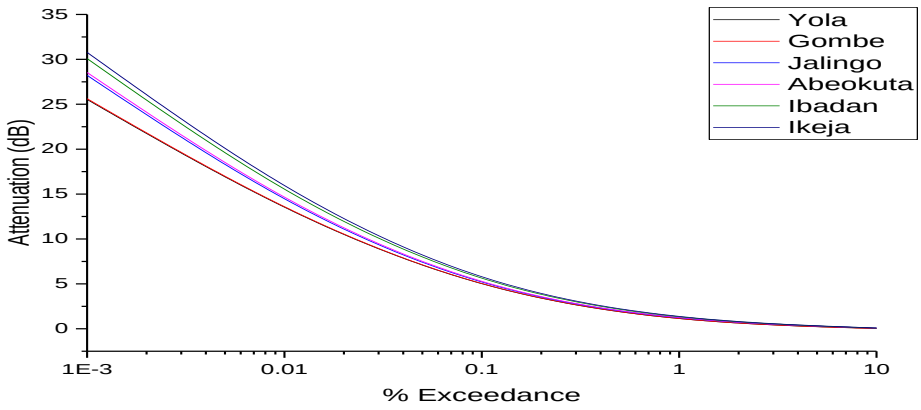

Figure 4.26: Rain attenuation at 11 GHz and 23° elevation angle for horizontal polarisation

From Figure 4.26, the rain attenuation at Ku-band downlink frequency for Yola, Gombe, Jalingo, Abeokuta, Ibadan and Ikeja at 0.01% time exceedance was observed to be 22.61 dB, 22.70 dB, 23.16 dB, 23.45 dB, 24.88 dB and 25.58 dB respectively.

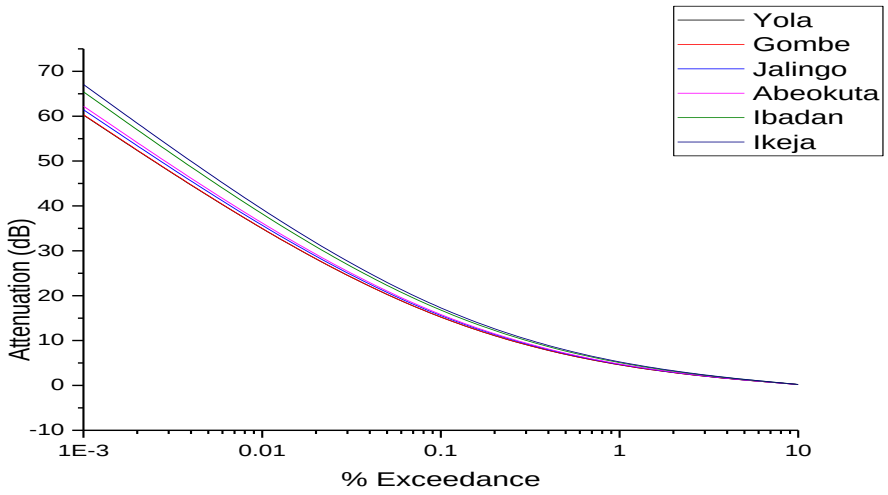

Figure 4.27: Rain attenuation at 14 GHz and 23° elevation angle for horizontal polarisation

From Figure 4.27, the rain attenuation computed at Ku-band downlink frequency for Yola, Gombe, Jalingo, Abeokuta, Ibadan and Ikeja at 0.01% time exceedance was 36.32 dB, 36.40 dB, 37.14 dB, 37.66 dB, 39.88 dB and 40.99 dB respectively.

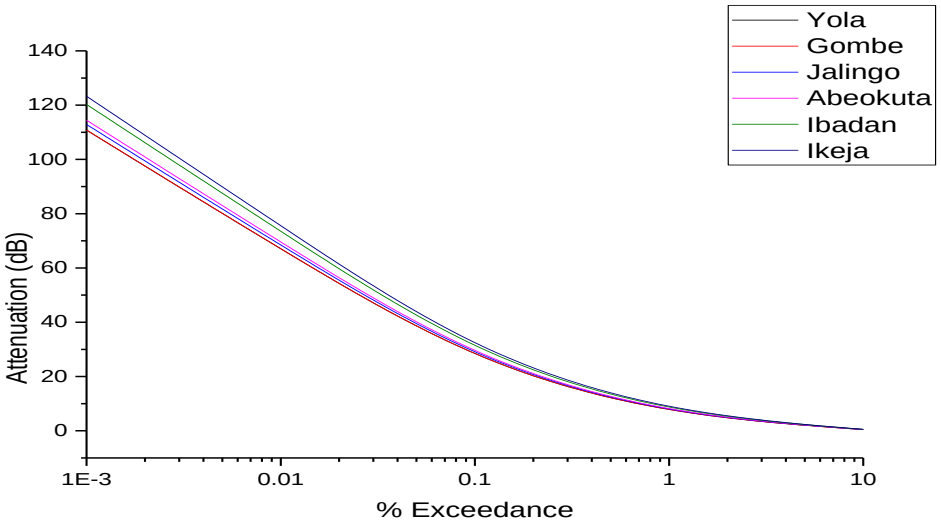

Figure 4.28: Rain attenuation at 20 GHz and 23° elevation angle for horizontal polarisation

From Figure 4.28, the rain attenuation at Ku-band downlink frequency for Yola, Gombe, Jalingo, Abeokuta, Ibadan and Ikeja at 0.01% time exceedance was observed to be 67.08 dB, 67.10 dB, 68.48 dB, 69.56 dB, 73.52 dB and 75.58 dB respectively.

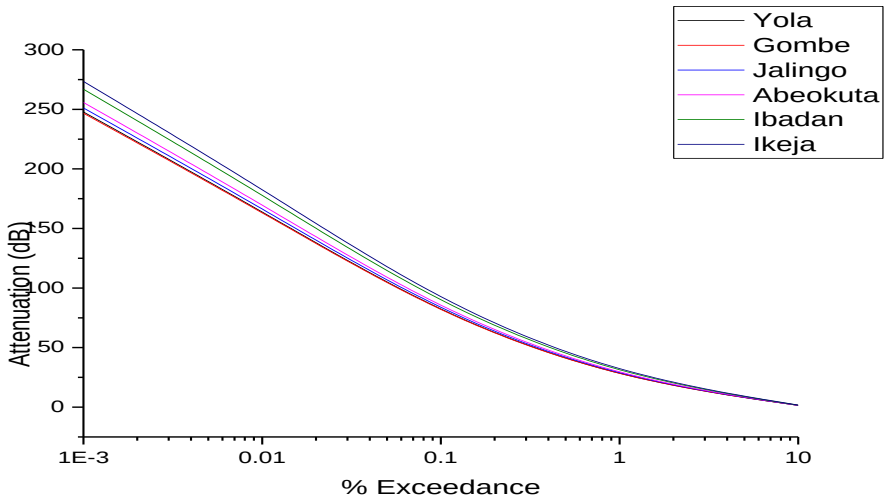

Figure 4.29: Rain attenuation at 40 GHz and 23° elevation angle for horizontal polarisation

From Figure 4.29, the rain attenuation computed at Ku-band downlink frequency for Yola, Gombe, Jalingo, Abeokuta, Ibadan and Ikeja at 0.01% time exceedance was 164.63 dB, 163.87 dB, 167.19 dB, 170.56 dB, 178.91 dB and 183.75 dB respectively.

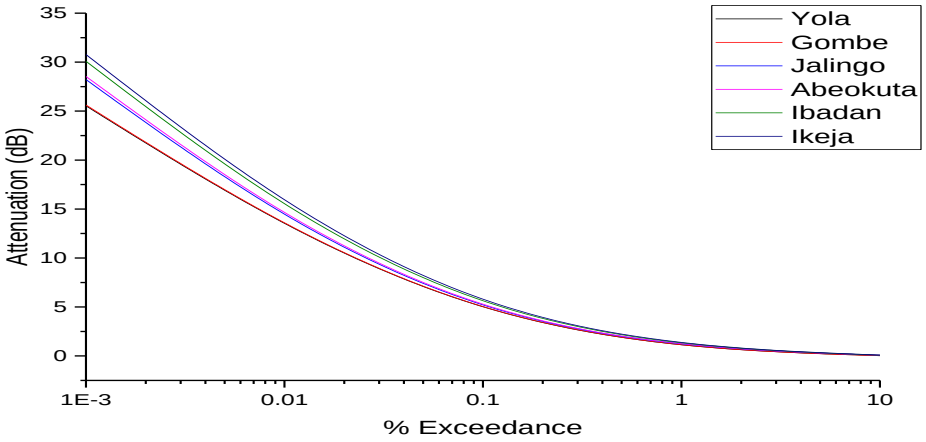

Figure 4.30: Rain attenuation at 11 GHz and 23° elevation angle for vertical polarisation

From Figure 4.30, the rain attenuation computed at Ku-band downlink frequency for Yola, Gombe, Jalingo, Abeokuta, Ibadan and Ikeja at 0.01% time exceedance was 19.83 dB, 19.88 dB, 20.29 dB, 20.56 dB, 21.80 dB and 22.42 dB respectively.

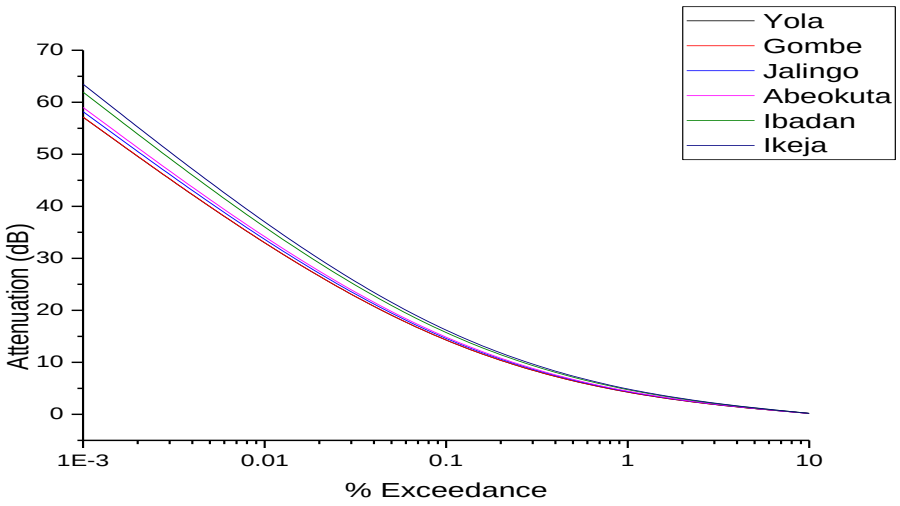

Figure 4.31: Rain attenuation at 14 GHz and 23° elevation angle for vertical polarisation.

From Figure 4.31, the rain attenuation at Ku-band downlink frequency for Yola, Gombe, Jalingo, Abeokuta, Ibadan and Ikeja at 0.01% time exceedance was observed to be 32.05 dB, 32.06 dB, 32.71 dB, 33.21 dB, 35.08 dB and 36.04 dB respectively.

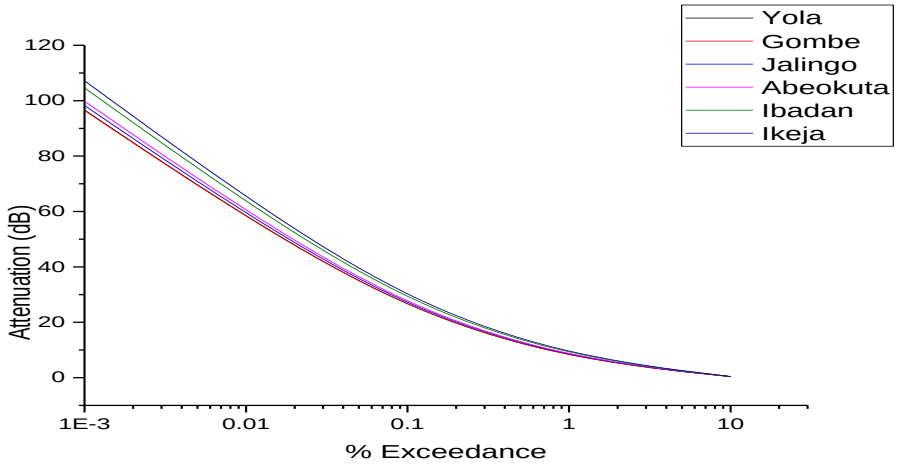

Figure 4.32: Rain attenuation at 20 GHz and 23° elevation angle for vertical polarisation

From Figure 4.32 , the rain attenuation at Ku-band downlink frequency for Yola, Gombe, Jalingo, Abeokuta, Ibadan and Ikeja at 0.01% time exceedance was observed to be 57.59 dB, 57.51 dB, 58.68dB, 59.71 dB, 62.93 dB and 64.67 dB respectively.

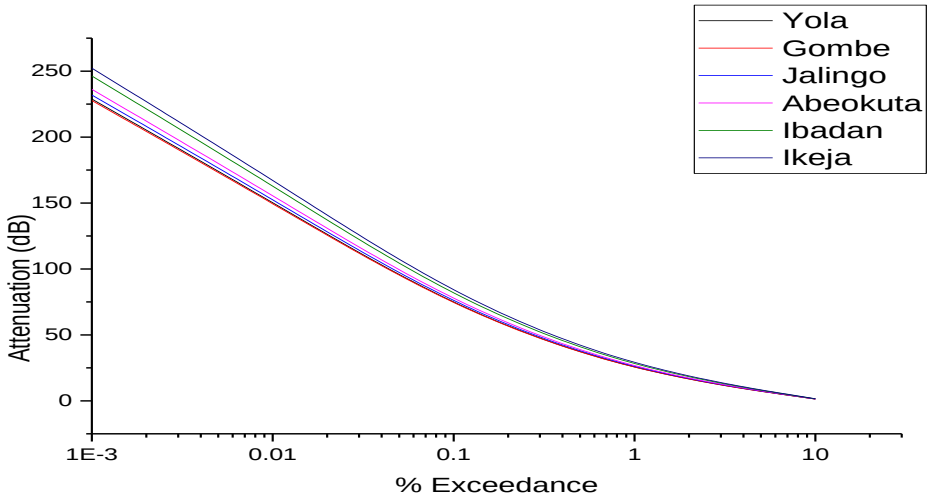

Figure 4.33: Rain attenuation at 40 GHz and 23° elevation angle for vertical polarisation

From figure, the rain attenuation at Ku-band downlink frequency for Yola, Gombe, Jalingo, Abeokuta, Ibadan and Ikeja at 0.01% time exceedance was observed to be 150.68 dB, 149.88 dB, 152.91 dB, 156.10 dB, 163.58 dB and 167.99 dB respectively.

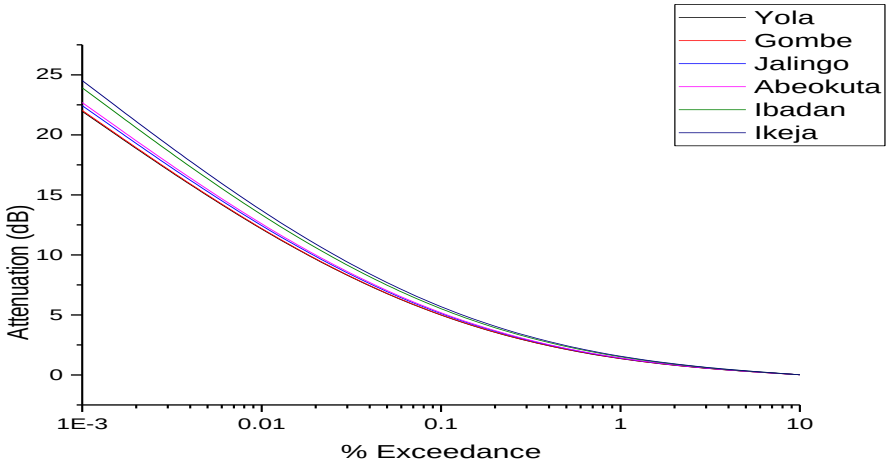

Figure 4.34: Rain attenuation at 11 GHz and 23° elevation angle for circular polarisation

The rain attenuation graph computed at Ku-band downlink frequency for Yola, Gombe, Jalingo, Abeokuta, Ibadan and Ikeja at 0.01% time exceedance was 21.20 dB, 21.27 dB, 21.70 dB, 21.99 dB, 23.32 dB and 23.98 dB respectively.

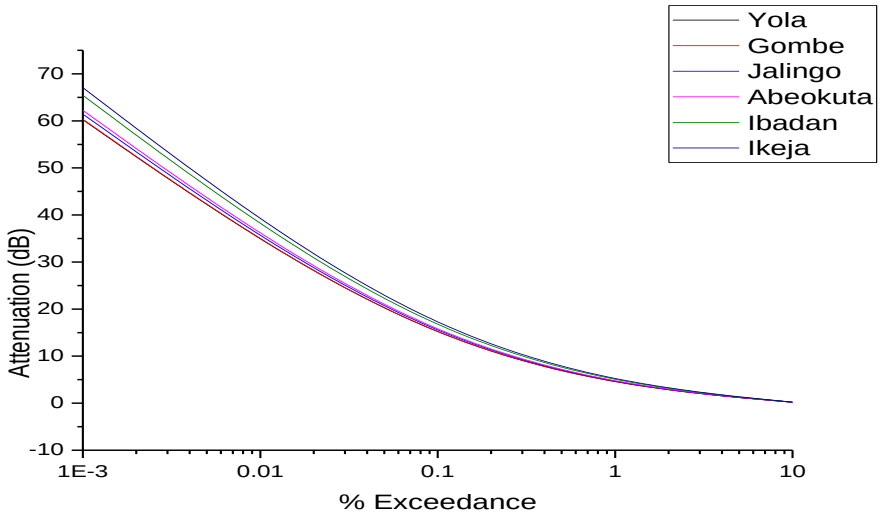

Figure 4.35: Rain attenuation at 14 GHz and 23° elevation angle for circular polarisation

From Figure 4.35, the rain attenuation computed at Ku-band downlink frequency for Yola, Gombe, Jalingo, Abeokuta, Ibadan and Ikeja at 0.01% time exceedance was 34.01 dB, 34.05 dB, 34.74 dB, 35.25 dB, 37.28 dB and 38.31 dB respectively

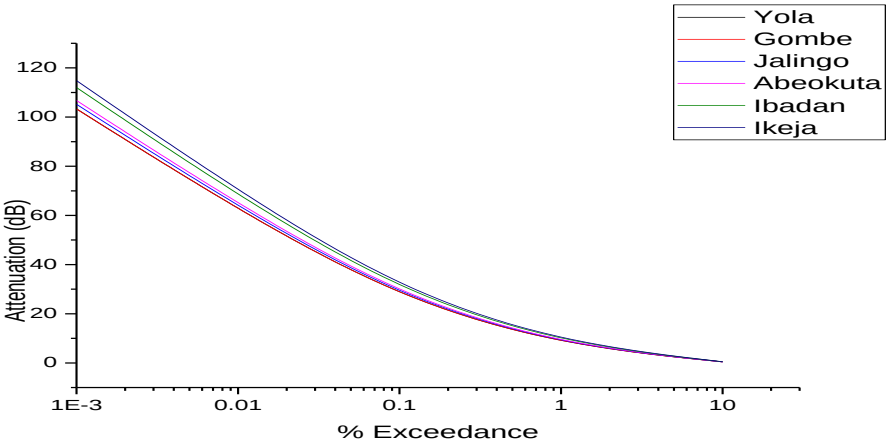

Figure 4.36: Rain attenuation at 20 GHz and 23° elevation angle for circular Polarisation

From Figure 4.36, the rain attenuation at Ku-band downlink frequency for Yola, Gombe, Jalingo, Abeokuta, Ibadan and Ikeja at 0.01% time exceedance was observed to be 62.07 dB, 62.03 dB, 63.31 dB, 64.36 dB, 67.92 dB and 69.81 dB respectively.

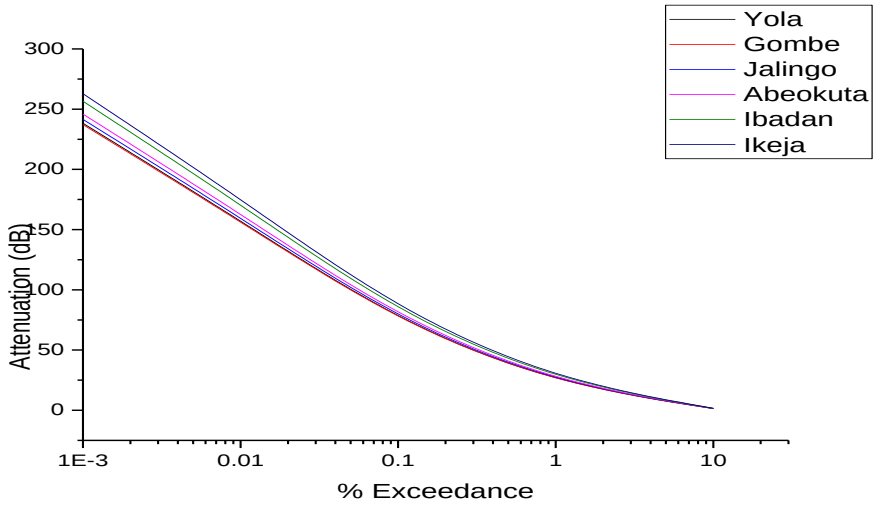

Figure 4.37: Rain attenuation at 40 GHz and 23° elevation angle for circular polarisation

From Figure 4.37, the rain attenuation computed at Ku-band downlink frequency for Yola, Gombe, Jalingo, Abeokuta, Ibadan and Ikeja at 0.01% time exceedance was 157.63 dB, 156.85 dB, 160.03 dB, 163.31 dB, 171.22 dB and 175.85 dB respectively.

From the computed attenuation, it is observed that horizontal polarisation had the highest amount of attenuation at all operational frequencies.This was followed by circular polarisation, while vertical polarisation had the least amount of attenuation for both the uplink and downlink frequencies of Ku- and Ka-bands for all the elevation angles considered for this study. From the values of attenuation predicted at time percentage of 0.01% which is equivalent to 99.99% availability (about 53 min outage in a year), signal is possible at 55° and 42.5° elevation angles but impossible at 23° elevation angle at the Ku

band. It is also impossible at the three elevation angles for the Ka-band, there by implying total signal fade out during rainfall events in all the stations.

CHAPTER FIVE

5.0 CONCLUSION AND RECOMMENDATIONS

5.1 Conclusion

Rain attenuation characteristics for satellite links at Ku and Ka-bands in the Northeast and Southwest Nigeria have been investigated for links to Nigeria Communication Satellite-1 replacement based on local input data. Rain attenuation values were computed for 0.001%-10% time exceedance using ITU-R P.618-12 rain attenuation model for Adamawa, Gombe, Taraba, Lagos, Ogun and Oyo States of Nigeria respectively.

Rainfall rate which is one of the inputs in the calculation of rain attenuation were evaluated and the results show that higher rainfall rates of 108.2 mm/h, 99.7 mm/h and 104.8 mm/h were recorded in Lagos, Ogun and Oyo respectively compared to that experienced in Adamawa, Gombe, and Taraba having rain rates of 90.34 mm/h, 94.4 mm/h and 96.2 mm/h respectively. Consequently more rain attenuation was experienced in the Southwestern states (Lagos, Ogun and Oyo States) than in Northeastern States (Adamawa, Gombe, and Taraba) for both downlink and uplink frequencies of the Ku and Ka-bands. Rain attenuation at 0.01 percentage time excedance for the Northeastern States ranged between 10.22 dB and 20.24 dB at 55° elevation angle, 11.89 dB and 24.01 dB at 42.5° elevation angle and between 19.83 dB to 37.14 dB at 23° elevation angle at the Ku-band, while the rain attenuation computed for the Southwestern states ranged between 10.60 dB to 22.34 dB at 55° elevation angle, 12.85 dB to 26.44 dB at 42.5° elevation angle and 20.56 dB to 40.99 dB at 23° for exceedance time percentage of 0.01% at Ku-band. For the Ka-band, attenuation for the Northeastern States varied from 33.79 dB to 110.10 dB at 55°elevation angle, 37.88 dB to 121.03 dB at 42.5° elevation angle and between 57.51 dB to 167.19 dB at 23° elevation angle. The rain attenuation computed for the Southwestern states ranged between 44.63 dB and 122.11 dB at 55°elevation angle, 40.39 dB and 133.48 dB at 42.5° elevation angle and between 59.71 dB and 183.75 dB at 23° elevation angle for same 0.01% exceedance time percentage in all the stations.From the values of rain attenuation predicted for 0.01% time exceedance, availability of signal is possible at 42.5° and 55° elevation angles but impossible at 23° elevation angle at Ku-band. At Ka-band, the predicted rain attenuation values for 0.01% time exceedance have shown that availability of signal is impossible at all three elevation angles, which implies total signal fade out during such rain fall events in the region.

5.2 Recommendations

- More rain rate and rain attenuation models should be employed for the analysis of rain rate and rain attenuation for better comparison and better results.
- The predicted rain attenuation calculated in this work should be considered by satellite communication engineers when designing satellite communication systems in the locations studied in order to have a more efficient transmission.
- Rain gauge should be installed in every part of the country so as to get more accurate rainfall and rainfall rate measurements.

REFERENCES

Adimula, I.A. (2015) Rainfall parameters in Ilorin and their application to microwave radio propagation, PhD Thesis, University of Ilorin, Ilorin.

Adrian, J. T. (2011) A study of the raindrop size Distribution and its effect on Microwave Attenuation, PhD Thesis,Electronics and Electrical Engineering, University of Bath.

Ajayi, G. O., (1990) Rain drop characteristics during a tropicalthunderstorm and monsoon rainfall at Ile-Ife. Antenna Tele-commun., 39, 515–522

Ajayi, G. O. and Ofoche, B. C (1984) Some tropical rainfall rate characteristics at Ile-Ife for microwave and millimeter wave applications, Journal of Climate & Applied Meteorology, vol. 23, no. 4, pp. 562–567,

Ajewole, M. O. (2011) Radio and rain: Friends and foes 62nd inaugural lecture delivered at Federal University of Technology, Akure; June 21, 2011.

Akinyemi,O.I, Alonge, T.A, Ojo O.I, Ogunkunle,O.(2018) Geo- spartial trend mapping of annual climate variable for south west Nigeria.Acta Techn Corviniensis bull Eng 12:14-105.

Chebil, J. and Raihman, T. A. (1999) Development of the one–minute Rain Rate Contour Maps for Microwave Applications in Malaysia Peninsula, Electronics Letters, Vol.35, No.20 pp. 1772–1774.

COST 235, (1996) Radiowave propagation effects on next-services terrestrial telecommunications systems

Crane, R. K. (1982) Attenuation due to rain-A mini-review, IEEE Transactions on Antenna and Propagation, pp. 751-752.

Emiliani, L.D.(2014)Development of rain-attenuation and rain-rate maps for satellite system design in the Ku and Ka bands in Colombia. Antennas and Propagation Magazine, IEEE, 2004. 46(6): p. 54-68.

Freeman, R. L. (2013) Radio System Design for Telecommunications -Hoboken, New Jersey, John Willey and Sons, Inc, pp. 112-120.

Hassan, A.A. (2014): Indicators for the signal Degradation and Optimization of Automotive Radar Sensors under Adverse Weather Conditions PhD Dissertation submitted to Elekrotechnik and InformationsTechnik der Technishen, University of Darmstadt.

Igwe, K.C, Oyedum, O.D, Ajewole, M.O, and Aibinu, A.M. 188 (2019).52-61.
Evaluation of some rain attenuation prediction models for satellite communication at Ku
and Ka band. Journal of Atmospheric and Solar-Terrestrial Physics..

Islam Md Rafiqul, Md Moktarul, Alam, Ali Kodhm, Lwas and Sarah,Yasmin Muhamad, (2018): Rain distribution of rain distribution for satellite link design based on long time measurement in Malaysia. Harmattan Weather. American Journal of Scientific and Industrial Research. ISSN: 2153-649X.

ITU-R, "Propagation data and prediction methods required for the design of Earth-space Telecommunication system", Rec. ITU-R P.618-9, 2009.

ITU-R, "Rain height model for prediction methods", Rec. ITU-RP.839-3, (2001)

ITU-R P. 618-12, (2012) Rain height model for prediction methods international Telecommunication Unioin. Geneva, Switzerland

Ivanous, G. and Serdega, D. (2006) Rain Intensity Influence on to Microwave Line Payback Terms, Electronics and Electrical Engineering, No. 6(70), pp. 60 - 64.

Khandaker, L.B. and Mohammad, M.R. (2014) Performance Analysis of Rain Fades on Microwave Earth-to-Sattelite Links in Bangladesh. International Journal of Engineering and Technology, Volume 4, No 7

Malinga, S. J. Owolawi, P. S., and Afullo, T. J. O. (2013) Estimation of Rain Attenuation at C, Ka, Ku and V Bands for Satellite Links in South Africa, PIERS Proceedings, Taipei, March 25-28, 2013, pp. 948 – 958

Moupfouma, F. (1984), Improvement of rain attenuation prediction method for terrestrial microwave links, *IEEE Trans. Antennas Propag.*, **32**(12), 1368– 1372

Moupfouma, F. (2009) Electromagnetic wave attenuation due to rain: A prediction model for terrestrial or L.O.S SHF/EHF radio communication links, Journal of infrared milli tera HZ waves, vol. 30, no. 3, pp. 622-632.

Moupfouma, F. and Martin, S. (2009) Modeling of the rainfall rate cumulative distribution for design of satellite and terrestrial communication systems, International Journal of Satellite Communication, 13 (2), pp. 105-115.

Moupfouma, F. and Martin, S. (2015) Modeling of the rainfall rate cumulative distribution for design of satellite and terrestrial communication systems, International Journal of Satellite Communication, 13 (2), pp. 105-115.

Moupfouma, F. and Tiffon .J.(2014) Raindrop size distribution from microwave scattering measurements in equatorial and tropical climates. Electron let 18.1012-1014

Ojo, J.S. (1977) Relation between measured radar reflectivity and surface rainfall, Monthly weather Review, vol. 115, pp. 1053-1070.

Ojo, J.S and Ajewole, M.O. (2011) Rain rate and rain attenuation prediction for satellite communication in Ku and Ka bands over Nigeria Progress in electromagnetic research, B. pp. 217-223.

Ojo, J.S and Olurotimi, E.O.(2014) modeling freezing height level for satellite link communication:Durban South Africa IEEE African PP 342-347

Ojo, J.S. (2015) Rain rate statistics and fade distributions at ka- and ku band frequencies locations, The Nigerian Journal of Space Research, vol. 10, pp. 72-80.

Omotoso, T. V. (2016) Studies of Propagation impairments for Fixed satellite communication links at the microwave frequencies in Nigeria, PhD Thesis submitted to Covenant University Otta, Nigeria.

Panagopoulos, A.D. Arapoglou, P-D. M. And Gottis, P. G. (2004) Satellite Communications at Ku, Ka, and V bands: Propagation impairments and mitigation techniques", IEEE Communications Surveys and Tutorials, 6(3) pp. 2 – 14.

Parth Panch and Rutvij Josh, (2016).Performance Analysis and Simulation of Rain Attenuation Models at 12–40 GHz Band for an Earth Space Pathover Indian Cities 7th International Conference on Communication, Computing and Virtualization 2016

Rahim, A.K. Al-tabatabaie, F. Abdulrahman, A.Y. (2013). Fade Margins Prediction for Broadband Fixed Wireless Access (BFWA) from Measurement in Tropics. Progress in Electromagnetics Research C, Vol. 11, 199-212

Ryde, J.W. (1946). The attenuation and radar echoes produced at centimetre wavelengths by various meteorological phenomena; in Meteorological Factors in Radio-wave propagation", Physical Society: London, England, pp. 169-188.

Tokay, D.A. and Short,(2015) Evidence from tropical raindrop spectra of the origin of rain from stratiform versus convective cloudsJ. Appl. Meteorol., pp. 355-371

Rice, P. and Holmberg, N. (1973) Cummulative Time Statistics of surface-Point Rainfall Rates", IEEE Transactions on Communications, vol. 21, no. 10, pp. 1131-1136.

Salonen, E. T. and Poiares-Baptisa, J. P. V. (1997) A new global rainfall rate model"Proceedings of the 10th International Conference on Antenna and propagation. pp. 182 – 185.

Shoewu, O. and Edeko, F.O., (2011). Microwave Signal Attenuation at 7.2GHz in Rain and Harmattan Weather. American Journal of Sceientific and Industrial Research. ISSN: 2153-649X

Vaclav Kvicera and Martin Grabner,(2013).Rain attenuation at 58 GHz: Prediction Versus Long-term Trial Results.EURASIP Journal on Wireless Communications and Networking archive. Volume 2007 Issue 1, January 2013, Pages 46-46

APPENDICES

Appendix A : 33 years average rainfall for the study area.

Month	Yola	Gombe	Jalingo	Abeokuta	Ibadan	Ikeja
Jan	0.0	0.0	0.0	5.2	5.5	18.2
Feb	0.0	0.0	0.0	25.0	40.0	35.7

Mar	1.2	3.8	3.6	93.0	75.5	72.3
Apr	10.4	13.1	19.0	126.0	123.7	137.1
May	55.6	71.5	74.3	64.4	163.0	204.9
Jun	130.7	172.5	169.2	158.9	186.8	280.1
Jul	211.9	238.3	257.4	214.1	191.4	208.7
Aug	255.2	291.2	297.9	264.0	145.0	212.0
Sep	136.8	142.1	167.3	172.4	205.2	194.1
Oct	18.6	17.1	24.1	245.0	184.2	168.4
Nov	0.0	2.1	0.0	21.0	24.9	83.9
Dec	0.0	0.0	0.0	13.0	8.3	20.3
Total	820.4	951.7	1012.8	1402	1353.5	1635.7

Appendix B1 :33 years total rainfall events for Yola

State capital (Yola)	Total rainfall per year (mm)	Total no of rainfall event per year	Average total rainfall per year (mm)	Total no of months with rain per year	Driest month without rain

1985	808.1	74	2.21	8	1,2,11,12
1986	829.0	64	2.27	8	1,2,11,12
1987	800.8	59	2.19	6	1,2,3,4,11,12
1988	806.2	64	2.20	7	1,2,3,11,12
1989	841.6	59	2.31	7	1,2,3,11,12
1990	775.0	67	2.12	8	1,2,11,12
1991	794.4	63	2.18	8	1,2,11,12
1992	745.5	55	2.04	8	1,2,11,12
1993	704.7	52	1.93	7	1,2,3,11,12
1994	850.6	59	2.33	7	1,2,3,11,12
1995	893.8	63	2.45	7	1,2,3,11,12
1996	884.1	59	2.42	7	1,2,3,11,12
1997	877.4	59	2.40	7	1,2,3,11,12
1998	895.7	63	2.45	7	1,2,3,11,12
1999	815.6	59	2.23	7	1,2,3,11,12
2000	804.5	49	2.20	6	1,2,3,4,11,12
2001	886.6	61	2.43	7	1,2,3,11,12
2002	883.1	58	2.42	8	1,2,11,12
2003	839.6	60	2.30	7	1,2,3,11,12
2004	800.9	48	2.19	7	1,2,3,11,12
2005	739.5	58	2.03	7	1,2,3,11,12
2006	844.9	57	2.31	8	1,2,3,11,12
2007	848.2	54	2.33	7	1,2,3,11,12
2008	772.4	57	2.11	7	1,2,3,11,12
2009	766.9	51	2.10	7	1,2,3,11,12
2010	750.7	61	2.06	7	1,2,3,11,12
2011	885.0	52	2.42	7	1,2,3,11,12
2012	928.3	54	2.54	8	1,2,11,12
2013	727.8	53	1.99	7	1,2,3,11,12
2014	783.1	51	2.15	7	1,2,3,11,12
2015	730.4	46	2.00	7	1,2,3,11,12
2016	868.4	62	2.38	7	1,2,3,11,12
2017	980.6	59	2.44	7	1,2,3,11,12

Total rainfall for 33 years = 27163 mm.

Appendix B3: 33 years total rainfall events for Gombe

State capital (Gombe)	Total rainfall per year (mm)	Total no of rainfall event per year	Average total rainfall per year	Total no of months with rain per year	Driest month without rain
1985	905.3	62	2.48	8	1,2,11,12
1986	960.5	65	2.63	8	1,2,11,12
1987	955.7	60	2.62	6	1,2,3,4,11,12
1988	917.8	59	2.51	7	1,2,3,,11,12
1989	937.8	59	2.57	7	1,2,3,,11,12
1990	954.1	68	2.61	8	1,2,3,,11,12
1991	968.5	59	2.65	9	1,2,3,,11,12
1992	963.8	58	2.69	8	1,2,3,,11,12
1993	921.3	69	2.52	7	1,2,3,,11,12
1994	961.7	61	2.63	7	1,2,3,,11,12
1995	943.3	61	2.58	7	1,2,3,,11,12
1996	951.1	68	2.61	7	1,2,3,,11,12
1997	952.8	65	2.61	7	1,2,3,,11,12
1998	932.1	74	2.55	7	1,2,3,,11,12
1999	968.3	82	2.65	7	1,2,3,,11,12
2000	951.1	68	2.61	6	1,2,3,,11,12
2001	971.8	70	2.66	7	1,2,3,,11,12
2002	934.4	69	2.55	8	1,2,3,,11,12
2003	934.9	65	2.56	7	1,2,3,,11,12
2004	962.2	74	2.64	7	1,2,3,,11,12
2005	967.5	76	2.64	6	1,2,3,,11,12
2006	961	77	2.63	8	1,2,3,,11,12
2007	931.1	71	2.55	7	1,2,3,,11,12
2008	949.2	67	2.60	7	1,2,3,,11,12
2009	971.9	73	2.66	7	1,2,3,,11,12
2010	973.2	68	2.67	7	1,2,3,,11,12
2011	969.3	72	2.66	7	1,2,3,,11,12
2012	989.8	69	2.71	8	1,2,3,,11,12
2013	928.3	65	2.54	7	1,2,3,,11,12
2014	9489	64	2.60	7	1,2,3,,11,12
2015	954.6	66	2.62	6	1,2,3,,11,12
2016	941.6	67	2.58	7	1,2,3,,11,12
2017	952.8	62	2.60	8	1,2,3,,11,12

Total rainfall for 33 years = 31387 mm

Appendix B4 : 33 years total rainfall events for Jalingo

Sate capital (Jalingo)	Total rainfall per year (mm)	Total no of rainfall event per year	Average total rainfall per year	Total no of months with rain per year	Driest month without rain
1985	1227.7	77	3.37	8	1,2,11,12
1986	1132.3	69	3.10	8	1,2,11,12
1987	1214.7	70	3.33	8	1,2,11,12
1988	1127.4	66	3.08	7	1,2,10,11,12
1989	1078.5	63	2.95	7	1,2,3,11,12
1990	1145.5	75	3.14	7	1,2,10,11,12
1991	1034.9	69	2.84	7	1,2,10,11,12
1992	1125.5	57	3.08	7	1,2,10,11,13
1993	1055.9	53	2.89	8	1,2,11,12
1994	1109.9	59	3.04	8	1,2,11,12
1995	1186.0	64	3.25	8	1,2,11,12
1996	1130.9	59	3.09	7	1,2,4,11,12
1997	1075.0	59	2.95	8	1,2,11,14
1998	1218.2	63	3.34	8	1,2,11,15
1999	1145.9	59	3.14	7	1,2,4,11,12
2000	804.50	49	2.20	7	1,2,4,11,12
2001	886.60	61	2.43	7	1,2,4,11,12
2002	883.10	58	2.42	8	1,2,11,12
2003	839.60	60	2.30	8	1,2,11,12
2004	800.90	48	2.19	6	1,2,3,10,11,12
2005	739.50	58	2.03	7	1,2,3,11,12
2006	844.90	57	2.31	7	1,2,3,11,12
2007	848.20	54	2.33	7	1,2,10,11,12
2008	772.40	57	2.11	7	1,2,3,11,12
2009	766.90	51	2.10	7	1,2,3,11,13
2010	750.70	61	2.06	7	1,2,3,11,14
2011	885.0	52	2.42	7	1,2,3,11,15
2012	1322.1	54	3.61	7	1,2,3,11,16
2013	1039.7	53	2.85	7	1,2,3,11,17
2014	1048.6	51	2.87	7	1,2,3,11,18
2015	1027	46	2.81	7	1,2,3,11,19
2016	1106.5	62	3.03	7	1,2,10,11,12
2017	1047.4	59	2.87	7	1,2,3,11,19

Total rainfall for 33 years = 33421.9 mm

Appendix B5:33 years total rainfall events for Abeokuta.

State capital (Abeokuta)	Total rainfall per year (mm)	Total no of rainfall event per year	Average total rainfall per year	Total no of months with rain per year	Driest month without rain
1985	1321.3	108	4.05	11	1
1986	1479.6	104	3.17	9	1,11,12
1987	1227.7	89	3.19	11	12
1988	1132.3	104	3.20	11	12
1989	1214.7	99	3.31	10	1,12
1990	1127.4	97	3.12	10	1,12
1991	1078.5	93	3.18	11	1
1992	1145.5	85	3.04	11	12
1993	1034.9	82	2.93	11	1
1994	1125.5	102	3.33	9	1,11,12
1995	1055.9	93	3.45	11	1
1996	1109.9	99	3.45	10	11,12
1997	1673.3	109	3.40	11	12
1998	1130.9	103	3.45	11	1
1999	1738.2	112	3.23	11	12
2000	1218.2	104	3.20	11	1
2001	1145.9	101	3.43	11	1
2002	1322.1	108	3.42	10	1,12
2003	1097.4	100	3.30	11	12
2004	1008.6	88	3.19	11	12
2005	1039.7	98	3.03	10	1,12
2006	1109.0	107	3.31	11	12
2007	1145.9	109	3.33	11	1
2008	1047.4	102	3.11	12	Nil
2009	1140.0	111	3.10	12	Nil
2010	1450.5	91	3.06	11	12
2011	1379.9	102	3.40	9	1,11,12
2012	1533.9	98	4.19	11	1
2013	1326.5	108	3.63	10	1,12
2014	1244.1	99	3.41	10	1,12
2015	1259.5	101	3.44	11	1
2016	1233.6	93	3.38	10	1,12
2017	1201.4	91	3.29	10	1,12

Total rainfall for 33 years = 40580.2 mm

Appendix B6: 33 years total rainfall events for Ibadan

State capital (Ibadan)	Total rainfall per year (mm)	Total no of rainfall event per year	Average total rainfall per year	Total no of months with rain per year	Driest month without rain
1985	1608.5	114	4.41	11	1
1986	1297.7	83	3.56	10	1,12
1987	1285.8	113	3.52	9	1,11,12
1988	1408.0	122	3.85	12	Nil
1989	1344.4	115	3.68	9	1,11,12
1990	1283.9	115	3.52	12	Nil
1991	1369.3	112	3.75	11	1
1992	1072.7	110	2.93	9	1,2,12
1993	1257.3	111	3.44	11	1
1994	1002.7	103	2.75	11	12
1995	1534.9	114	4.21	10	1,12
1996	1647.9	117	4.50	10	11,12
1997	1195.3	114	3.27	11	2
1998	920.6	86	2.52	11	1
1999	1814.9	115	4.97	11	12
2000	1197.7	97	3.27	9	2,11,12
2001	1289.7	91	3.53	11	1
2002	1515.3	112	4.15	10	1,12
2003	1469.3	111	4.03	11	12
2004	1327.4	97	3.63	11	12
2005	1226.2	89	3.36	11	1
2006	1447.0	109	3.96	11	12
2007	1247.4	109	3.42	11	1
2008	1765.0	110	4.82	10	1,11
2009	1916.4	104	5.25	11	12
2010	1520.1	127	4.16	11	12
2011	1586.1	103	4.35	10	1,12
2012	1377.2	117	3.76	10	1,12
2013	1203.2	97	3.30	11	12
2014	1056.4	106	2.89	12	Nil
2015	1058.2	89	2.89	12	Nil
2016	1028.3	103	2.82	11	12
2017	1393.3	365	3.82	12	Nil

Total rainfall for 33 years = 44668.1mm

Appendix B7: 33 years total rainfall events for Ikeja

State capital (Ikeja)	Total rainfall per year (mm)	Total no of rainfall event Per year	Average total rainfall per year	Total no of months with rain per year	Driest month without rain
1985	1052.9	104	2.88	11	3
1986	1015.2	84	2.78	11	12
1987	1688.7	93	4.63	10	1,12
1988	1927.0	99	5.27	12	Nil
1989	1368.9	94	3.75	9	1,2,12
1990	1610.1	88	4.41	11	1
1991	1671.8	108	4.58	12	Nil
1992	1188.4	90	3.25	11	1
1993	1671.5	101	4.58	11	1
1994	1085.9	91	3.21	12	Nil
1995	1629.8	133	4.47	11	1
1996	1535.0	97	4.19	12	Nil
1997	1835.8	96	5.03	11	1
1998	926.5	76	2.54	11	12
1999	1506.2	117	4.13	12	Nil
2000	1125.2	88	3.07	11	12
2001	1392.1	106	3.81	12	Nil
2002	1802.3	115	4.94	11	2
2003	1692.1	104	4.64	12	Nil
2004	1699.2	103	4.64	12	Nil
2005	1483.9	98	4.07	10	1,12
2006	1516.9	112	4.16	12	Nil
2007	1539.8	97	4.22	10	1,2
2008	1553.7	113	4.25	11	2
2009	1393.2	88	3.82	12	Nil
2010	1669.5	110	4.57	9	1,2,11
2011	1748.0	102	4.79	10	1,12
2012	1555.8	114	4.25	10	2,12
2013	1530.7	101	4.19	11	12
2014	2117.1	118	5.80	12	Nil
2015	1182.6	97	3.23	11	12
2016	1205.5	90	3.29	10	1,2
2017	1690.4	101	4.63	11	1

Total rainfall for 33 years = 49611.71mm

Appendix B2: Key indicating number representing each month

Months	Jan	Feb	Mar	Apr	May	Jun	Jul	Aug	Sep	Oct	Nov	Dec
Number	1	2	3	4	5	6	7	8	9	10	11	12

APPENDIX C

THE PREDICTED RAIN ATTENUATION FOR THE STUDY AREA

Tables C1- C6: Variation of rain attenuation with respect to % time exceedance for the study area in horizontal, vertical and circular polarisations at 55° elevation angle

Table C1 Variation of rain attenuation for horizontal polarisation at Ku-band

	At 11 GHz					At 14 GHz				
	0.001	0.01	0.1	1	10	0.001	0.01	0.1	1	10
Yola	21.96	11.66	4.32	0.95	0.01	35.28	19.79	7.75	1.80	0.02
Gombe	22.03	11.71	4.34	0.95	0.01	35.35	19.84	7.77	1.80	0.02
Jalingo	22.59	12.04	4.48	0.99	0.01	36.26	20.41	8.02	1.87	0.02
Abeokuta	23.19	12.40	4.62	1.02	0.01	37.29	21.06	8.23	1.94	0.03
Ibadan	24.26	13.03	4.89	1.09	0.01	38.92	22.09	8.75	2.05	0.03
Ikeja	23.52	12.59	4.71	1.04	0.01	37.66	21.29	8.40	1.96	0.03

Table C2 Variation of rain attenuation for horizontal polarisation at Ka-band

	At 20 GHz					At 40 GHz				
	0.001	0.01	0.1	1	10	0.001	0.01	0.1	1	10
Yola	64.05	38.50	16.15	4.02	0.06	158.12	105.51	49.14	13.57	0.21
Gombe	65.62	39.55	16.64	4.15	0.06	161.73	108.20	50.53	13.99	0.22
Jalingo	68.39	41.42	17.51	4.39	0.06	169.15	113.75	53.40	14.86	0.24
Abeokuta	67.45	40.78	17.21	4.31	0.06	166.97	112.11	52.55	14.60	0.23
Ibadan	70.43	42.80	18.16	4.57	0.07	173.30	116.87	55.02	15.35	0.25
Ikeja	66.88	40.40	17.04	4.26	0.06	162.89	109.06	50.98	14.12	0.22

Table C3 Variation of rain attenuation for vertial polarisation at Ku-band

	At 11 GHz					At 14 GHz				
	0.001	0.01	0.1	1	10	0.001	0.01	0.1	1	10

Yola	19.09	9.97	3.64	0.79	0.01	25.94	14.05	5.31	1.19	0.02
Gombe	19.56	10.25	3.75	0.81	0.01	26.58	14.43	5.47	1.23	0.02
Jalingo	20.36	10.72	3.94	0.86	0.01	27.70	15.11	5.75	1.30	0.02
Abeokuta	20.07	10.55	3.87	0.84	0.01	27.31	14.88	5.66	1.27	0.02
Ibadan	21.01	11.10	4.09	0.90	0.01	28.52	15.61	5.97	1.35	0.02
Ikeja	20.04	10.53	3.86	0.84	0.01	27.10	14.75	5.60	1.26	0.02

Table C4 Variation of rain attenuation for vertial polarisation at Ka-band

	At 20 GHz					At 40 GHz				
	0.001	0.01	0.1	1	10	0.001	0.01	0.1	1	10
Yola	55.66	32.92	13.59	3.33	0.05	145.31	96.02	44.29	12.11	0.20
Gombe	56.98	33.79	13.99	3.43	0.05	148.60	98.44	45.53	12.48	0.20
Jalingo	59.45	35.43	14.74	3.63	0.05	155.49	103.55	48.14	13.27	0.21
Abeokuta	58.65	34.90	14.49	3.57	0.05	153.51	102.08	47.39	13.04	0.21
Ibadan	61.09	36.52	15.24	3.77	0.05	159.18	106.30	49.55	13.69	0.22
Ikeja	57.83	34.35	14.24	3.50	0.05	149.39	99.03	45.82	12.57	0.20

Table C5 Variation of rain attenuation for circular polarisation at Ku-band

	At 11 GHz					At 14 GHz				
	0.001	0.01	0.1	1	10	0.001	0.01	0.1	1	10
Yola	20.27	10.67	3.92	0.85	0.01	32.50	18.06	7.01	1.61	0.02
Gombe	20.78	10.97	4.04	0.88	0.01	33.29	18.55	7.22	1.66	0.02
Jalingo	21.62	11.46	4.24	0.93	0.01	34.65	19.40	7.58	1.76	0.02
Abeokuta	21.31	11.28	4.17	0.91	0.01	34.17	19.10	7.45	1.72	0.02
Ibadan	22.32	11.88	4.41	0.97	0.01	35.69	20.05	7.86	1.83	0.02
Ikeja	21.32	11.29	4.17	0.91	0.01	33.99	18.99	7.40	1.71	0.02

Table C6 Variation of rain attenuation for circular polarisation at Ka-band

	At 20 GHz					At 40 GHz				
	0.001	0.01	0.1	1	10	0.001	0.01	0.1	1	10
Yola	59.64	35.55	14.79	3.65	0.05	151.71	100.75	46.70	12.83	0.20
Gombe	61.08	36.51	15.24	3.77	0.05	155.16	103.30	48.01	13.23	0.21
Jalingo	63.69	38.26	16.04	3.99	0.06	162.34	108.64	50.75	14.06	0.22
Abeokuta	62.82	37.68	15.77	3.91	0.06	160.23	107.08	49.95	13.81	0.22
Ibadan	65.52	39.49	16.61	4.14	0.06	166.24	111.57	52.27	14.52	0.23
Ikeja	62.12	37.20	15.56	3.86	0.05	156.13	104.03	48.38	13.34	0.21

Tables 7- 12: Show variation of rain attenuation with respect to % time exceedance for the study area in horizontal, vertical and circular polarisations at 42.5° elevation angle

Table C7 Variation of rain attenuation for horizontal polarisation at Ku-band

	At 11 GHz					At 14 GHz				
	0.001	0.01	0.1	1	10	0.001	0.01	0.1	1	10
Yola	24.99	13.22	4.89	1.11	0.02	39.58	22.08	8.62	2.05	0.04
Gombe	25.62	13.59	5.04	1.14	0.02	40.54	22.68	8.87	2.12	0.05
Jalingo	28.81	14.82	5.35	1.27	0.08	45.39	24.60	9.36	2.34	0.15
Abeokuta	28.40	14.58	5.25	1.24	0.08	44.76	24.21	9.20	2.30	0.15
Ibadan	29.75	15.35	5.56	1.32	0.08	46.79	25.44	9.71	2.44	0.16
Ikeja	28.41	14.58	5.26	1.24	0.08	44.55	24.09	9.15	2.28	0.15

Table C8. Variation of rain attenuation for horizontal polarisation at Ka-band

	At 20 GHz					At 40 GHz				
	0.001	0.01	0.1	1	10	0.001	0.01	0.1	1	10
Yola	72.03	43.07	18.01	4.60	0.10	172.62	114.19	52.82	14.93	0.38
Gombe	73.77	44.23	18.54	4.75	0.11	176.46	117.03	54.27	15.38	0.39
Jalingo	82.05	47.62	19.40	5.19	0.36	194.19	124.49	56.03	16.57	1.25
Abeokuta	80.92	46.89	19.07	5.10	0.35	191.73	122.73	55.16	16.29	1.23
Ibadan	84.49	49.20	20.11	5.40	0.37	198.88	127.85	57.70	17.11	1.30
Ikeja	80.27	46.47	18.88	5.04	0.34	187.21	119.51	53.56	15.77	1.19

Table C9 Variation of rain attenuation for vertial polarisation at Ku-band

	At 11 GHz					At 14 GHz				
	0.001	0.01	0.1	1	10	0.001	0.01	0.1	1	10
Yola	22.22	11.60	4.23	0.94	0.02	35.37	19.48	7.50	1.77	0.04
Gombe	22.77	11.92	4.36	0.98	0.02	36.21	20.00	7.72	1.82	0.04

Jalingo	25.60	12.98	4.62	1.08	0.06	40.51	21.67	8.14	2.01	0.13
Abeokuta	25.23	12.78	4.54	1.06	0.06	39.96	21.34	8.00	1.97	0.12
Ibadan	26.42	13.45	4.81	1.13	0.07	41.69	22.37	8.43	2.09	0.13
Ikeja	25.22	12.77	4.54	1.06	0.06	39.67	21.17	7.92	1.95	0.12

Table C10 Variation of rain attenuation for vertical polarisation at Ka-band

	At 20 GHz					At 40 GHz				
	0.001	0.01	0.1	1	10	0.001	0.01	0.1	1	10
Yola	64.28	37.93	15.65	3.95	0.09	163.28	107.32	49.32	13.85	0.35
Gombe	64.19	37.88	15.63	3.94	0.09	162.47	106.73	49.02	13.76	0.34
Jalingo	69.69	39.69	15.87	4.17	0.28	174.25	110.32	49.03	14.32	1.07
Abeokuta	70.80	40.39	16.18	4.26	0.29	177.64	112.71	50.21	14.70	1.10
Ibadan	74.27	42.61	17.16	4.54	0.31	185.55	118.33	52.98	15.58	1.17
Ikeja	76.14	43.81	17.69	4.70	0.32	190.19	121.64	54.61	16.11	1.21

Table C11 Variation of rain attenuation for circular polarisation at Ku-band

	At 11 GHz					At 14 GHz				
	0.001	0.01	0.1	1	10	0.001	0.01	0.1	1	10
Yola	24.12	12.71	4.68	1.05	0.02	38.16	21.20	8.24	1.96	0.04
Gombe	24.18	12.75	4.70	1.06	0.02	38.20	21.23	8.25	1.96	0.04
Jalingo	26.63	13.57	4.85	1.14	0.07	41.83	22.46	8.46	2.10	0.13
Abeokuta	26.94	13.74	4.92	1.16	0.07	42.39	22.79	8.60	2.13	0.14
Ibadan	28.40	14.58	5.25	1.24	0.08	44.57	24.11	9.15	2.28	0.15
Ikeja	29.12	14.99	5.42	1.29	0.08	45.69	24.78	9.43	2.36	0.15

Table C12 Variation of rain attenuation for circular polarisation at Ka-band

	At 20 GHz					At 40 GHz				
	0.001	0.01	0.1	1	10	0.001	0.01	0.1	1	10
Yola	68.77	40.90	17.01	4.32	0.10	170.24	112.44	51.93	14.65	0.37
Gombe	68.73	40.88	17.00	4.32	0.10	169.46	111.86	51.63	14.56	0.37
Jalingo	74.68	42.87	17.28	4.57	0.31	181.79	115.66	51.66	15.16	1.14
Abeokuta	75.81	43.59	17.60	4.67	0.32	185.26	118.12	52.88	15.55	1.17
Ibadan	79.62	46.04	18.69	4.99	0.34	193.59	124.06	55.82	16.50	1.25
Ikeja	81.63	47.34	19.28	5.16	0.35	198.44	127.54	57.54	17.06	1.29

Tables C13- C18: Show variation of rain attenuation with respect to % time exceedance for the study area in horizontal, vertical and circular polarisations at 23° elevation angle

Table C13: Variation of rain attenuation for horizontal polarisation at Ku-band

	At 11 GHz					At 14 GHz				
	0.001	0.1	0.10	1	10	0.001	0.1	0.10	1	10
Yola	41.80	22.61	8.58	2.11	0.11	63.92	36.32	14.48	3.75	0.21
Gombe	41.94	22.70	8.62	2.12	0.11	64.05	36.40	14.51	3.75	0.21
Jalingo	42.70	23.16	8.81	2.18	0.11	65.22	37.14	14.84	3.85	0.21
Abeokuta	43.18	23.45	8.93	2.21	0.12	66.03	37.66	15.07	3.91	0.22
Ibadan	45.54	24.88	9.54	2.37	0.13	69.50	39.88	16.05	4.19	0.23
Ikeja	46.69	25.58	9.83	2.45	0.13	71.24	40.99	16.55	4.33	0.24

Table C14 Variation of rain attenuation for horizontal polarisation at Ka-band

	At 20 GHz					At 40 GHz				
	0.001	0.01	0.1	1	10	0.001	0.01	0.1	1	10
Yola	110.79	67.08	28.49	7.85	0.46	247.74	164.63	76.75	23.22	1.50
Gombe	110.81	67.10	28.50	7.86	0.46	246.71	163.87	76.36	23.09	1.49
Jalingo	112.86	68.48	29.15	8.05	0.47	251.19	167.19	78.07	23.65	1.53
Abeokuta	114.46	69.56	29.66	8.21	0.48	255.72	170.56	79.81	24.23	1.57
Ibadan	120.27	73.52	31.53	8.77	0.52	266.92	178.91	84.13	25.67	1.67
Ikeja	123.29	75.58	32.50	9.07	0.54	273.38	183.75	86.64	26.51	1.73

Table C15 Variation of rain attenuation for vertical polarisation at Ku-band

	At 11 GHz					At 14 GHz				
	0.001	0.01	0.1	1	10	0.001	0.01	0.1	1	10
Yola	37.15	19.83	7.42	1.80	0.09	57.14	32.05	12.61	3.22	0.18
Gombe	37.24	19.88	7.44	1.81	0.09	57.16	32.06	12.62	3.22	0.18
Jalingo	37.93	20.29	7.61	1.85	0.10	58.20	32.71	12.90	3.30	0.18
Abeokuta	38.39	20.56	7.73	1.88	0.10	59.00	33.21	13.12	3.36	0.18

Ibadan	40.45	21.80	8.24	2.02	0.11	61.96	35.08	13.93	3.59	0.20
Ikeja	41.48	22.42	8.50	2.09	0.11	63.49	36.04	14.36	3.71	0.20

Table C16 Variation of rain attenuation for vertical polarisation at Ka-band

	At 20 GHz					At 40 GHz				
	0.001	0.01	0.1	1	10	0.001	0.01	0.1	1	10
Yola	96.63	57.59	24.08	6.53	0.38	228.84	150.68	69.61	20.87	1.33
Gombe	96.50	57.51	24.04	6.52	0.38	227.75	149.88	69.20	20.73	1.32
Jalingo	98.27	58.68	24.59	6.68	0.39	231.88	152.91	70.74	21.24	1.36
Abeokuta	99.80	59.71	25.06	6.82	0.40	236.21	156.10	72.37	21.77	1.40
Ibadan	104.62	62.93	26.55	7.27	0.42	246.33	163.58	76.21	23.04	1.48
Ikeja	107.21	64.67	27.37	7.52	0.44	252.27	167.99	78.48	23.79	1.54

Table C17 Variation of rain attenuation for circular polarisation at Ku-band

	At 11 GHz					At 14 GHz				
	0.001	0.01	0.1	1	10	0.001	0.01	0.1	1	10
Yola	39.45	21.20	7.99	1.96	0.10	60.26	34.01	13.46	3.46	0.19
Gombe	39.56	21.27	8.02	1.96	0.10	60.33	34.05	13.48	3.46	0.19
Jalingo	40.29	21.70	8.20	2.01	0.11	61.43	34.74	13.79	3.55	0.19
Abeokuta	40.76	21.99	8.32	2.04	0.11	62.23	35.25	14.01	3.61	0.20
Ibadan	42.97	23.32	8.88	2.19	0.12	65.43	37.28	14.90	3.86	0.21
Ikeja	44.06	23.98	9.16	2.27	0.12	67.05	38.31	15.36	3.99	0.22

Table C18. Variation of rain attenuation for circular polarisation at Ka-band

	At 20 GHz					At 40 GHz				
	0.001	0.01	0.1	1	10	0.001	0.01	0.1	1	10
Yola	103.34	62.07	26.16	7.15	0.42	238.28	157.63	73.16	22.03	1.41
Gombe	103.28	62.03	26.14	7.15	0.42	237.23	156.85	72.76	21.90	1.40
Jalingo	105.18	63.31	26.73	7.32	0.43	241.52	160.03	74.39	22.44	1.44
Abeokuta	106.75	64.36	27.22	7.47	0.44	245.96	163.31	76.07	22.99	1.48
Ibadan	112.03	67.92	28.89	7.97	0.47	256.62	171.22	80.15	24.35	1.58
Ikeja	114.83	69.81	29.78	8.24	0.49	262.82	175.85	82.54	25.14	1.63